Two-Stage Fault Location Detection Using PMU Voltage Measurements in Transmission Networks

Hao Wang

Thesis submitted to the faculty of Virginia Polytechnic Institute & State University in partial fulfillments of the requirements for the degree of

Master of Science
In
Electrical Engineering

Virgilio A. Centeno, Chair
Jaime De La Reelopez
Lamine Mili

May 11, 2015

Blacksburg, Virginia

Keywords: Fault Location, Transmission Network, PMU Voltage Measurements, Positive Sequence Network, Linear State Estimator

Two-Stage Fault Location Detection Using PMU Voltage Measurements in Transmission Networks

Hao Wang

ABSTRACT

Fault location detection plays a crucial role in power transmission network, especially on security, stabilization and economic aspects. Accurate fault location detection in transmission network helps to speed up the restoration time, therefore, reduce the outage time and improve the system reliability [1]. With the development of Wide Area Measurement System (WAMS) and Phasor Measurement Unit (PMU), various fault location algorithms have been proposed.

The purpose of this work is to determine, modify and test the most appropriate fault location method which can be implemented with a PMU only linear state estimator. The thesis reviews several proposed fault location methods, such as, one-terminal [2], multi-terminal [3]-[11] and travelling wavelets methods [12]-[13]. A Two-stage fault location algorithm using PMU voltage measurements proposed by Q. Jiang [14] is identified as the best option for adaption to operate with a linear state estimator. The algorithm is discussed in details and several case studies are made to evaluate its effectiveness. The algorithm is shown to be easy to implement and adapt for operation with a linear state estimator. It only requires a limited number of PMU measurements, which makes it more practical than other existing methods. The algorithm is adapted and successfully tested on a real linear state estimator monitored high voltage transmission network.

To my Father Yonggui Wang, my lifetime inspiration,

and my Mother Damei Qin

Acknowledgement

I would like to express my sincere gratitude to my advisor, Dr. Virgilio. A. Centeno for his significant role in my life. He provided me with guidance, inspiration, motivation, and continuous support throughout my Master studies. I am also grateful for his friendship and patience during these two years. In addition, I would like to thank my other committee members, Dr. Jaime De La Reelopez and Dr. Lamine Mili for their precious time and valuable advice during my graduate studies and on my thesis.

I am fortunate to have some amazing labmates as well as good friends in the power lab. I would like to thank Duotong Yang, Marvin, Marcos, Nawaf, Anna, for their kind help on both my study and my life.

Last, but not least, I would like to express my regards and thanks to my parents, my sister, Yu Qin, and my girlfriend Qian Li for their love, and support during all these years of my life. Their belief and encouragement only made my achievements ever possible.

Thank you all

Table of Contents

List of Figures

List of Tables

Chapter 1: Introduction

1.1 Introduction

The transmission network is a ligament between the generating units and the distribution systems. It is exposed to atmospheric conditions, and usually spreads hundreds of miles, which may across deserts, forests, mountains, hence the probability of experience a fault on transmission line is really high [15]. If the fault cannot be found and removed immediately, it will cause serious damage on the transmission line components and may eventually cause the system collapse. Therefore, it is necessary to have an accurate and fast fault location algorithm to locate the fault point. With the development of WAMS and PMU, various fault location detection algorithms have been proposed, which can be classified as three most classic methods:

(1) One-terminal Method

(2) Multi-terminal Method

(3) Travelling Wavelets Method

With the increase number of PMUs and readable available communication channels, PMU only linear state estimators are becoming a system monitoring option in modern control centers. A three phase PMU only linear state estimator was implemented at Dominion Virginia Power in 2013 which monitors the 500kV network [16]. A similar high voltage transmission network but positive sequence only linear state estimator is being implement at SCE [17]. Linear state estimators provide the advantage of simpler calculations and updates of 30 frames per second with possibility of increasing to 60 and 120 frames per second as communication channels improve. Several situational awareness algorithms for islanding, unbalance tracking and others have been proposed for implementation with the linear state estimator. This thesis proposes a fault location algorithm

which can provide a valuable situational awareness tool for system operators and a suitable companion tool for the topology processor required for a linear state estimator.

Each of the three classic methods for fault location described earlier has certain disadvantages for implementation as a companion tool for a linear state estimator. For example, one-terminal method may be affected by the fault resistance, thus the accuracy is being limited. Multi-terminal method is not affected by fault resistance, and has a higher accuracy than one-terminal method. However, it requires PMU voltage measurements at least at one-end of the terminals. In practice, due to the high cost of the PMUs and their installation, they cannot be installed with that high density in the transmission network. The traveling wavelets method has the highest accuracy, reliability and stability [18, 19], but it requires specialized equipment for data and it is not obtainable from PMUs. It also needs intensive simulations and it may be affected by the system operating conditions.

In [14], the authors developed a two-stage general fault location algorithm, which only uses a limited number of voltage measurements and the relative transfer impedance of the transmission network. The first stage narrows down the searching area by finding the suspicious fault buses. The second stage finds the exact fault distance along the transmission line. This algorithm looks easy to implement and only needs a limited number of PMU measurements as available with linear state estimators. However, when it comes to the actual implementation process, some details not covered in [14] have to be considered and will be discussed in this thesis. Not being affected by the fault resistance and fault type also make the algorithm practical when operating with linear state estimator.

A linear state estimator monitored system requires observability of the monitoring system. It has been shown by researchers at Virginia Tech that to achieve full observability, PMUs must

be placed in about 1/3 of the total number of buses throughout the system [20, 21]. By using those sparse PMU voltage measurements during a fault, a rough fault region can be detected by observing the voltage drops at the observed buses. Usually, the closer to the fault, the larger voltage change on magnitude can be observed. The algorithm proposed in [14] is able to further identify the suspicious fault buses in a suspicious fault region by only using those PMU voltage measurements. Once the suspicious fault buses are detected, the linear state estimator fault data can be used in this algorithm to locate the exact fault point. Theoretically, this algorithm should be able to operate well with the PMUs used to implement a linear state estimator. Several tests using standard IEEE models are presented in chapter 3. A real transmission network, which is monitored by PMU only linear state estimator, is used in chapter 4 to evaluate the performance of the algorithm.

1.2 Thesis contributions and organization

1.2.1 Thesis contributions

The basic theory of this Two-stage fault location algorithm which will be discussed in Chapter 3 is based on the well-known concept of transfer impedance. In theory, the implementation of this approach is simple, however, several problems need to be addressed and solved for its implementation and adaption to work with a linear state estimator. The major contribution of this thesis is to adapt and evaluate the operation of the Two-Stage fault location algorithm, based on transfer impedance effect, when used with the system observability set of PMUs for linear state estimator.

1.2.2 Thesis Organization

Chapter 1 gives a brief introduction of the need of fault location algorithm and the existing three major fault location methods. Introduces a Two-Stage fault location algorithm which

proposed by Q. Jiang [14] and its major advantages compare to other exiting algorithms. Chapter 2 reviews the theory and algorithms behind the three major fault location methods.

Chapter 3 provides details of the Two-Stage fault location algorithm along with the implementations on several IEEE test systems and their testing results.

Chapter 4 shows the results of the implementation of the Two-Stage fault location algorithm on a real transmission network model.

Chapter 2: Review of the Classic Fault Location Methods

2.1 Review of One-terminal Method

2.1.1 Transmission Line Models

Overhead transmission lines can be characterized into three categories which are short lines, medium-length lines and long lines. Short lines usually have length less than 50 miles. Medium-length lines are usually from 50 miles to 150 miles. Lines above 150 miles can be characterized as long transmission lines [22]. Different line representation models are required for three classifications of overhead transmission lines. The equivalent circuit of short transmission line is shown in Figure 2.1. A nominal π-circuit is used to represent the medium-length transmission line, which is shown in Figure 2.2. However, the nominal π-circuit is no longer valid for long transmission lines, since it does not take into account the parameters of the line being uniformly distributed, it does not represent the actual transmission lines accurately as the length of the line increases. Thus, an equivalent π-circuit is introduced to represent the long transmission line shown in Figure 2.3.

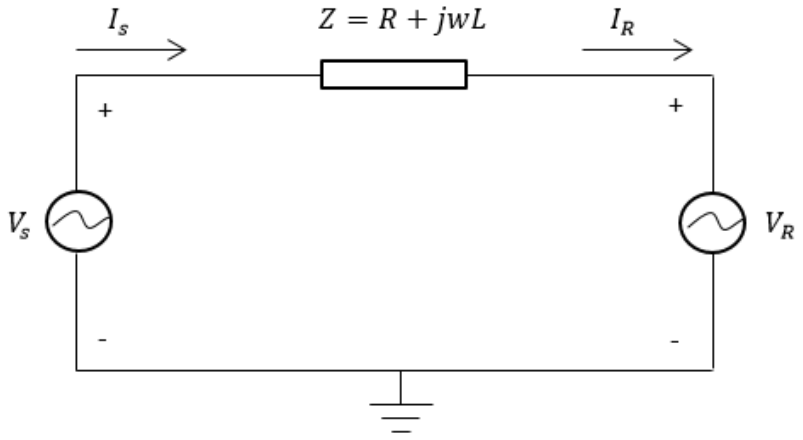

Figure 2.1: Equivalent circuit of a short transmission line.

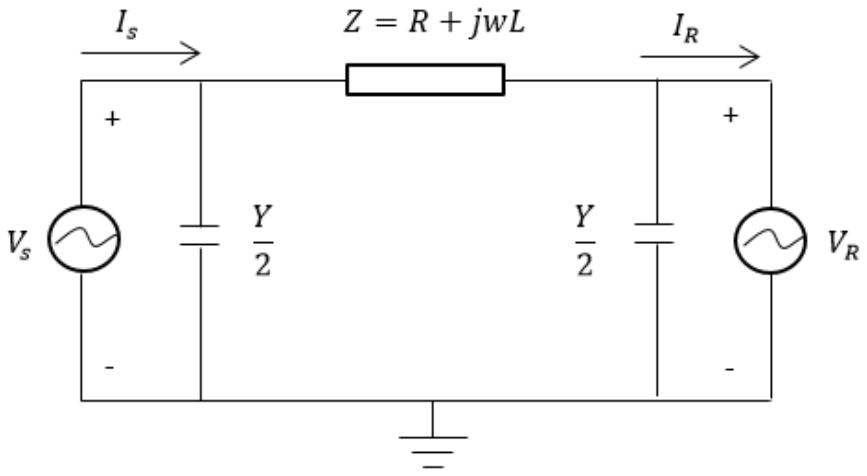

Figure 2.2: Nominal π-circuit of a medium-length transmission line.

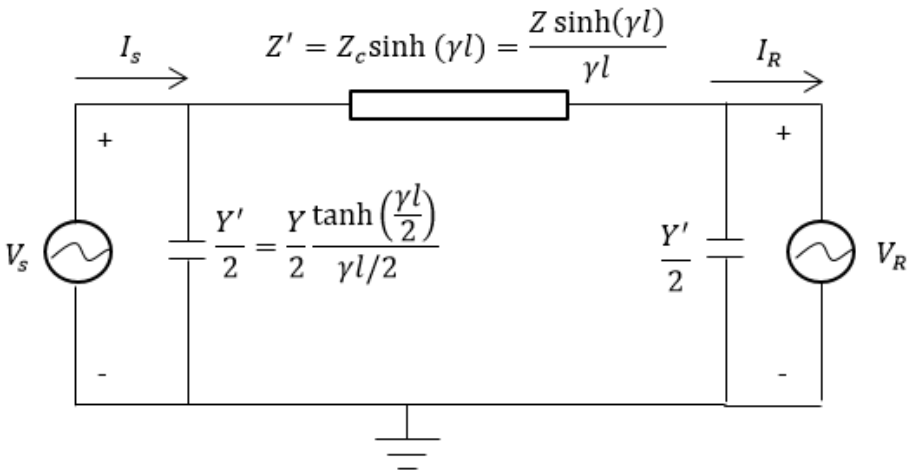

Figure 2.3: Equivalent π-circuit for long transmission line.

Some important parameters that used to represent the transmission line models are defined as following:

$z = series\ impedance\ per\ unit\ length\ per\ phase$

$y = shunt\ admittance\ per\ unit\ length\ per\ phase\ to\ neutra$

$l = length\ of\ line$

$Z = zl = total\ series\ impedance\ per\ phase$

$Y = yl = total\ shunt\ admittance\ per\ phase\ to\ neutral$

$Z_c = characteristic\ impedance = \sqrt{z/y}$

$\gamma = propagation\ constant = \sqrt{zy}$

The above parameters will be used during the calculating process in One-terminal method as well as the new Two-stage fault location algorithm which will be discussed in chapter 3.

2.1.2 One-terminal Fault Location Method

One-terminal fault location method was first proposed by T. Takagi [2] in 1982. The basic idea is to use voltage and current data at one-end of the transmission line to calculate the distance to the fault point. Although it is a relatively old method, it is still being widely implemented in protective relaying equipment, and it also provides a solid foundation for later developed One-Terminal methods.

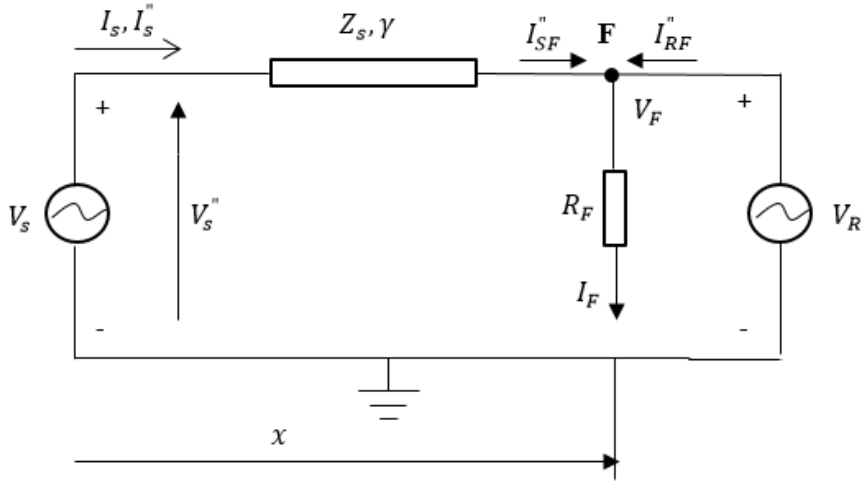

Figure 2.4: Fault in a single phase circuit.

For simplicity, a single phase circuit shown in Figure 2.4 is used to illustrate the calculation procedure.

The important parameters in Figure 2.4 are:

x: Distance to the fault point
V_S: Voltage of S-terminal
I_S: Current of S-terminal
V_F: Voltage at fault point
I_F: Fault current

$V_S^{"}$: Voltage difference between pre-fault and post-fault voltages at S-terminal

$I_S^{"}$: Current difference between pre-fault and post-fault currents at S-terminal

$I_{SF}^{"}$: Fault current from S-terminal

Z_S: Surge impedance

Z: Transmission line impedance per unit length

R_F: Fault resistance

γ: Propagation constant

Based Figure 2.4 and the parameters listed above, the following equations can be derived:

$$V_F = V_S \cosh(\gamma x) - Z_S I_S \sinh(\gamma x) \quad \text{……(2.1.1)}$$

$$I_{SF}^{"} = \frac{V_S^{"}}{Z_S} \sinh(\gamma x) - I_S^{"} \cosh(\gamma x) \quad \text{……(2.1.2)}$$

Two assumptions are made during the derivation of equations (2.1.1) and (2.1.2). One assumption is, for a sufficiently short transmission line (x is relatively short), $\tanh(\gamma x) \cong \gamma x$. Another assumption is the angle of fault current I_F and the angle of fault current from S-terminal $I_{SF}^{"}$ are identical.

Fault in a single phase circuit in Figure 2.5(a) can be represented by two sets of circuits, one is pre-fault load flow component circuit, and another one is fault component circuit during fault, which are shown in Figure 2.5(b) and 2.5(c) respectively.

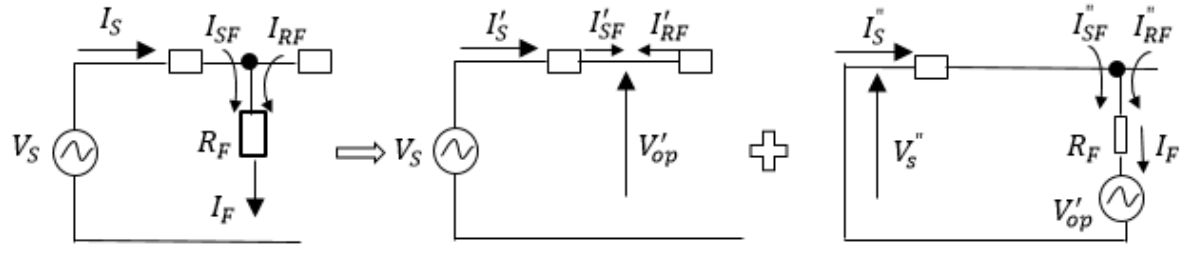

(a) A single phase circuit with a fault (b) Load flow component (c) Fault component

Figure 2.5: Two sets of circuits for a fault in a single phase.

From the fault point, the voltage V_F can be derived.

$$V_F = I_F R_F = (I_{SF} + I_{RF})R_F = \left(I_{SF}^{"} + I_{RF}^{"}\right)R_F \quad \text{……(2.1.3)}$$

$$I_F = I_{SF}^{"} \cdot \dot{\zeta} \quad \text{……(2.1.4)}$$

$$\dot{\zeta} = \zeta \cdot e^{j\theta}, \ \ where\ \theta = \arg\left(\frac{I_F}{I_{SF}^{"}}\right) \quad \text{……(2.1.5)}$$

From equations (2.1.1), (2.1.2), (2.1.3), (2.1.4) and (2.1.5), the following equation (2.1.6) can be derived.

$$V_S - I_S Z_S \tanh(\gamma x) - \left(\frac{V_S^{"}}{Z_S}\tanh(\gamma x) - I_S^{"}\right)\zeta \cdot e^{j\theta} \cdot R_F = 0 \quad \text{……(2.1.6)}$$

From (2.1.6), ζ and R_F can be eliminated.

$$Im\left\{(V_S - I_S Z_S \tanh(\gamma x))\left(\frac{V_S^{"}}{Z_S}\tanh(\gamma x) - I_S^{"}\right)^{*} e^{-j\theta}\right\} = 0 \quad \text{……(2.1.7)}$$

The equation only contains the S-terminal data, only θ and x are unknowns. Once θ is given, the fault distance x can be calculated. θ is the phase angle difference between fault current I_F and the fault current from S-terminal $I_{SF}^{"}$, usually, this angle difference is close to zero. By using the assumptions that:

1) $\tanh(\gamma x) \cong \gamma x$
2) $\frac{V_S^{"}}{Z_S}\tanh(\gamma x) \ll I_S^{"}$
3) $\theta \cong 0$

The fault distance x can be calculated as:

$$x = \frac{Im\left(V_S I_S^{"*}\right)}{Im(Z I_S I_S^{"*})} \quad \text{……(2.1.8)}$$

From (2.1.8), the fault distance x only depends on one-terminal data (S-terminal in the case) and the transmission line impedance per unit length.

2.1.3 Summary

One-terminal method introduced in section 2.1.2 not only works for single-line-to-ground fault, but also works for line-to-line fault, double-line-to-ground fault and three-phase fault [23]-[25]. The overall accuracy of this one-terminal fault location method is good. However, the estimated fault location error may go up with the seriousness of faults, for example, a three phase fault may lead to a relatively high error. Besides, pre-fault loading conditions, as well as the current flowing through other phases along the transmission line will also have impact on the performance of the algorithm. The pivotal limitation on this method is that it only works well for the low fault resistance. But in reality, the fault resistance can be fairly high and the arcs are also highly non-linear, only deal with the low fault resistance is not practical. The aforementioned drawbacks make this one-terminal method failed to be adapted to operate with PMUs from a linear state estimator.

2.2 Review of Multi-terminal Method

2.2.1 Two-Terminal Fault Location Method

To improve the fault location detection accuracy, many two-terminal methods has been introduced [7], [26]-[28]. [26]-[28] applied two-terminal method by using the apparent line impedance and the synchronized current/voltage data at both ends of the line. However, the fault resistance, fault conditions, and pre-fault loading conditions all have impacts on the accuracy of the fault distance results. At certain fault conditions, the error is still relatively high.

The two-terminal method proposed by A. A. Girgis [7] can exemplify the most of the proposed two-terminal methods. This method is independent of the apparent line impedance and

it only uses locally synchronized three-phase voltages and currents [29] at both ends of the transmission line and the series line impedance matrix, Z_{abc} (assumed to be constant along the line). Furthermore, no assumptions on fault resistance and fault conditions are made. Consider the two-terminal line model in Figure 2.6.

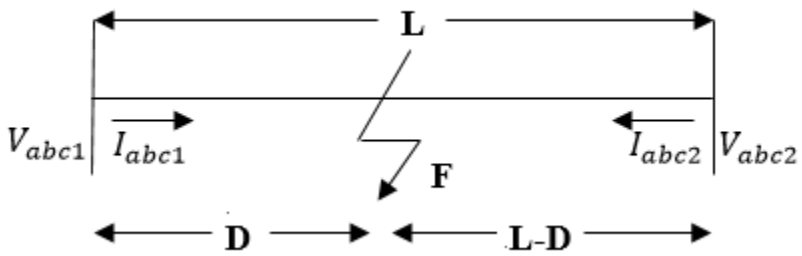

Figure 2.6: Two-Terminal line model.

V_{abc1}: Three-phase voltages at terminal 1
V_{abc2}: Three-phase voltages at terminal 2
I_{abc1}: Three-phase currents flow into the fault point from terminal 1
I_{abc2}: Three-phase currents flow into the fault point from terminal 2
L: Length of the transmission line
D: Fault distance from terminal 1
Z_{abc}: Three-phase series line impedance per mile

From Figure 6, three-phase voltages at terminal 1 and terminal 2 can be derived

$$V_{abc1} = V_{abc}^{F} + D \cdot Z_{abc} \cdot I_{abc1} \quad \text{……(2.2.1)}$$

$$V_{abc2} = V_{abc}^{F} + (L - D) \cdot Z_{abc} \cdot I_{abc2} \quad \text{……(2.2.2)}$$

Subtract (2.2.1) by (2.2.2) gives,

$$V_{abc1} - V_{abc2} + L \cdot Z_{abc} \cdot I_{abc2} = D \cdot Z_{abc}[I_{abc1} + I_{abc2}] \quad \text{……(2.2.3)}$$

Equation (2.2.3) can be written as three-phase vector form as:

$$\begin{bmatrix} Y_a \\ Y_b \\ Y_c \end{bmatrix} = \begin{bmatrix} M_a \\ M_b \\ M_c \end{bmatrix} D \rightarrow Y = MD \quad \text{……(2.2.4)}$$

Where,

$$Y_j = V_{j1} - V_{j2} + L \sum_{i=a,b,c} Z_{ji}\, I_{i2},\ (j = a, b, c) \quad \text{……(2.2.5)}$$

$$M_j = \sum_{i=a,b,c} Z_{ji}\, (I_{i1} + I_{i2}) \quad \text{……(2.2.6)}$$

Equation (2.2.4) consists of 3 complex equations (6 real equations) with only one unknown, D. The fault distance from terminal 1, D, can be calculated by using the least-squares method as following:

$$D = (M^{+}M)^{-1}M^{+}Y \quad \text{……(2.2.7)}$$

Where M^{+} is conjugate transpose of M.

This method has been widely mentioned in publications due to the advantages of that it is not affected by the fault resistance, fault type, and can provide higher accuracy than One-Terminal method. However, it is unable to be adapted to operate with PMU only linear state estimator due to that we usually don't have that many PMUs being placed in linear state estimator monitored system. Also, due to the high cost of PMUs and their installation, they cannot be installed at both terminals for every line in the transmission networks, especially the large ones.

2.2.2: Three-Terminal Fault Location Method

[7] gives a detailed Three-Terminal fault location method by using the synchronized data. Consider a three-terminal transmission line model in Figures 2.7, 2.8 and 2.9 below.

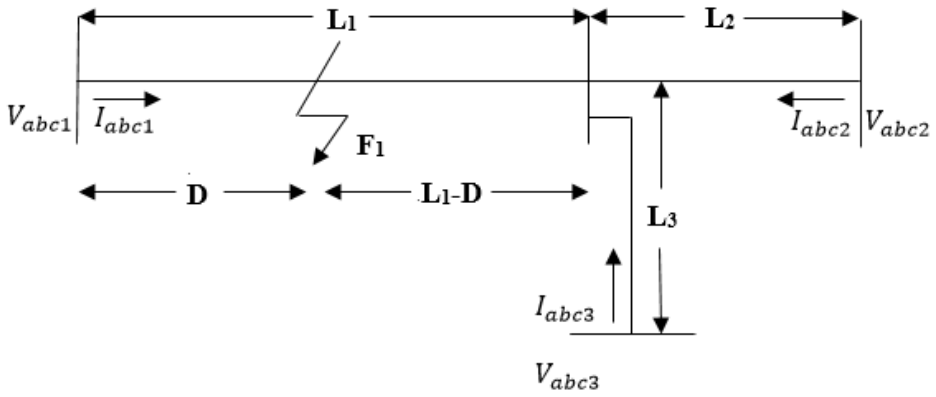

Figure 2.7: Three-terminal transmission line model when fault is at F_1.

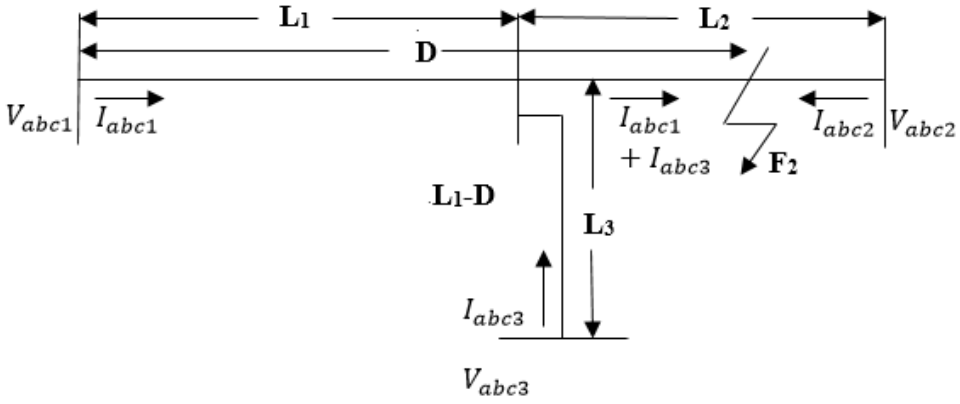

Figure 2.8: Three-terminal transmission line model when fault is at F_2.

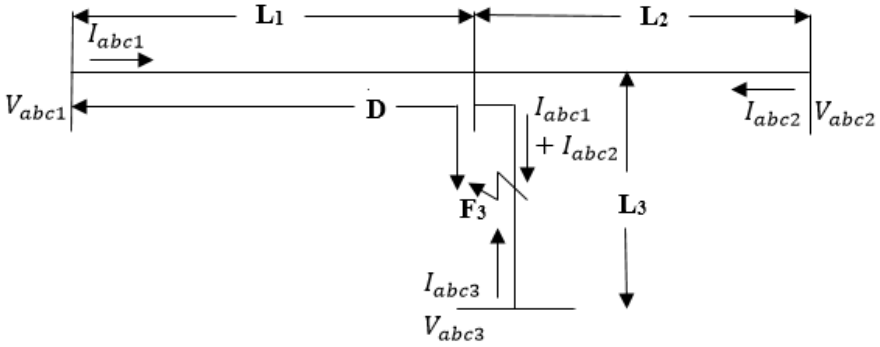

Figure 2.9: Three-terminal transmission line model when fault is at F_3.

The V and I terms in Figures 2.7, 2.8 and 2.9 have the same representations as in section 2.2.1. Z_{abc1}, Z_{abc2}, and Z_{abc3} represent the series line impedance matrix of L_1, L_2, and L_3 respectively. If the fault occurs at F_1 on section L_1 (shown in Figure 7), three-phase voltages at terminal 1, 2 and 3 can be derived as following:

$$V_{abc1} = V_{abc}^{F} + DZ_{abc1}I_{abc1} \quad \ldots\ldots(2.2.8)$$

$$V_{abc2} = V_{abc}^{F} + L_2Z_{abc2}I_{abc2} + (L_1 - D)Z_{abc1}(I_{abc2} + I_{abc3}) \quad \ldots\ldots(2.2.9)$$

$$V_{abc3} = V_{abc}^{F} + L_3Z_{abc3}I_{abc3} + (L_1 - D)Z_{abc1}(I_{abc2} + I_{abc3}) \quad \ldots\ldots(2.2.10)$$

From equations (2.2.8) and (2.2.9), the following equation can be derived.

$$V_{abc1} - V_{abc2} + (L_1Z_{abc1} + L_2Z_{abc2})I_{abc2} + L_1Z_{abc1}I_{abc3}$$

$$= DZ_{abc1}(I_{abc1} + I_{abc2} + I_{abc3}) \quad \ldots\ldots(2.2.11)$$

Similarly, from (2.2.8) and (2.2.10), the following equation can be derived.

$$V_{abc1} - V_{abc3} + (L_1Z_{abc1} + L_3Z_{abc3})I_{abc3} + L_1Z_{abc1}I_{abc2}$$

$$= DZ_{abc1}(I_{abc1} + I_{abc2} + I_{abc3}) \quad \ldots\ldots(2.2.12)$$

(2.2.11) can be expressed as (2.2.13):

$$\begin{bmatrix} Y1_a \\ Y1_b \\ Y1_c \end{bmatrix} = \begin{bmatrix} M_a \\ M_b \\ M_c \end{bmatrix} D \quad \ldots\ldots(2.2.13)$$

Where,

$$Y1_j = V_{j1} - V_{j2} + \sum_{k=a,b,c}\left(L_1Z_{1jk} + L_2Z_{2jk}\right)I_{k2} + L_1\sum_{k=a,b,c}Z_{1jk}I_{k3}$$

$$M_j = \sum_{k=a,b,c}(I_{k1} + I_{k2} + I_{k3})Z_{abc1}$$

$$j = a, b, c$$

Similarly, (2.2.12) can also be expressed as (2.2.14):

$$\begin{bmatrix} Y2_a \\ Y2_b \\ Y2_c \end{bmatrix} = \begin{bmatrix} M_a \\ M_b \\ M_c \end{bmatrix} D \quad \ldots\ldots(2.2.14)$$

Where,

$$Y2_j = V_{j1} - V_{j3} + \sum_{k=a,b,c}\left(L_1 Z_{1jk} + L_3 Z_{3jk}\right) I_{k3} + L_1 \sum_{k=a,b,c} Z_{1jk} I_{k3}$$

$$M_j = \sum_{k=a,b,c} (I_{k1} + I_{k2} + I_{k3}) Z_{abc1}$$

$$j = a, b, c$$

Each of Equations (2.2.13) and (2.2.14) consist of 3 complex equations (6 real equations) with only one unknown, D. The fault distance from terminal 1, D, can be calculated by using the least-squares method from (2.2.13):

$$D = (M^+ M)^{-1} M^+ Y1 \quad \ldots\ldots(2.2.15)$$

Or, it can also be calculated from (2.2.14)

$$D' = (M^+ M)^{-1} M^+ Y2 \quad \ldots\ldots(2.2.16)$$

If the fault occurs at F_2 on section L_2, assuming the line impedance per mile is constant, (2.2.13) still holds. However, (2.2.14) becomes:

$$\begin{bmatrix} Y2_a \\ Y2_b \\ Y2_c \end{bmatrix} = \begin{bmatrix} M_a \\ M_b \\ M_c \end{bmatrix} L_1 \quad \ldots\ldots(2.2.17)$$

If the fault occurs at F_3 on section L_3, assuming the line impedance per mile is constant, (2.2.14) still holds. However, (2.2.13) becomes:

$$\begin{bmatrix} Y1_a \\ Y1_b \\ Y1_c \end{bmatrix} = \begin{bmatrix} M_a \\ M_b \\ M_c \end{bmatrix} L_1 \qquad \ldots\ldots(2.2.18)$$

Based on previous calculations, (2.2.15) and (2.2.16) indicate the solution has the properties of:

1) If the fault occurs on section L_1. $D < L_1$ and $D' < L_1$.
2) If the fault occurs on section L_2. $D > L_1$ and $D' = L_1$.
3) If fault occurs on section L_3. $D = L_1$ and $D' > L_1$.

And no matter where the fault occurs, the fault distance D can be always found by solving equations (2.2.13) and (2.2.14). This Three-Terminal method is also independent of fault type, fault resistance. However, the method is still limited by the huge number of PMUs that need to be installed in the network, it is usually not possible in practice.

2.2.3 Summary

In section 2.2, the Two-Terminal and Three-terminal fault location methods have been reviewed. These two methods are not affected by the fault type, fault resistance, and insensitive to the pre-fault load conditions, hence, provide a more accurate fault location results. But the major drawback of these two methods is that they require a large number of PMUs to be installed in the transmission network. However, PMUs cannot be installed with such a high density due to the budget constraints. When dealing with PMU only linear state estimator, it is extremely beneficial to obtain the necessary data from minimum number of PMUs. Therefore, these two methods cannot be adapted to operate with PMUs from a linear state estimator.

2.3 Review of Traveling Wavelets Method

When sound wave hits objects, it will be reflected and refracted by the objects and forms an echo if the wave's magnitude is sufficiently large. The traveling wavelets method applies the same logic. In power system, voltages and currents can be regarded as traveling waves. When the traveling waves hit objects, they will also be reflected and refracted. A fault point can be regarded as one of those objects in power system. If a fault occurs on a transmission line, a transient wave can be generated and will travel back and forth between line terminals and the fault point. The fault distance can be calculated by measuring the traveling time of the wave. To illustrate this method, consider Figure 2.10 [30].

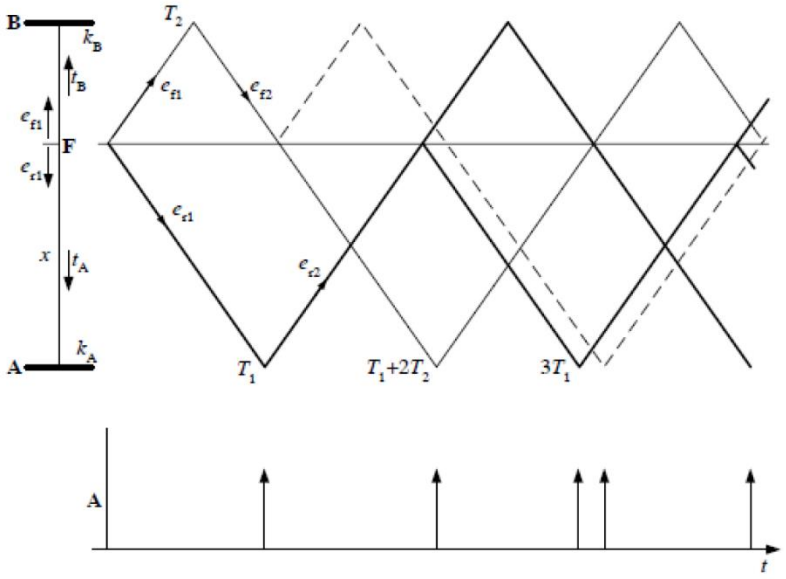

Figure 2.10: Traveling wave reflections and refractions for fault at F [26]. ([26] M. S. Sachdev, R. Agarwal, "A Technique for Estimating Line Fault Locations from Digital Relay Measurements," IEEE Trans. Power Del., Vol. PWRD-3, No. 1, Jan 1988, pp. 121-129. Used under fair use, 2015)

Assume a lossless transmission line with a length of l, and serge impedance of Z_s. A fault occurs at F, which has a distance of x from terminal A. The transient voltage waves e_{f1} and e_{f2} both travel at velocity of v. In Figure 2.10,

t_A: Transient wave travel time from fault point to terminal A

t_B: Transient wave travel time from fault point to terminal B

k_A: Reflection coefficient at terminal A, used to represent the wave amplitude

k_B: Reflection coefficient at terminal B, used to represent the wave amplitude

From [26], any fault point between terminal A and B with distance x from A should satisfy the following equation:

$$\frac{\partial e}{\partial x} = -L' \frac{\partial i}{\partial t} \quad \text{……(2.3.1)}$$

$$\frac{\partial e}{\partial x} = -C' \frac{\partial e}{\partial t} \quad \text{……(2.3.2)}$$

In above equations, the line resistance are neglected, L' is the line inductance, C' is the line capacitance, both in per unit length. The following solutions can be derived based on above equations:

$$e(x,t) = e_f(x - vt) + e_r(x + vt) \quad \text{……(2.3.3)}$$

$$i(x,t) = \frac{1}{Z_c}[e_f(x - vt) - e_r(x + vt)] \quad \text{……(2.3.4)}$$

Where, $Z_c = characteristic\ impedance = \sqrt{\frac{L'}{C'}}$ and $v = propagation\ velocity = \sqrt{\frac{1}{L'C'}}$. e_f is the forward voltage wave, e_r is the reverse voltage wave. Current waves (i_f, i_r) are similar to voltage waves. With GPS time synchronization, the traveling time t_A and t_B can be obtained at terminals A and B very precisely. Thus, the fault distance x can be calculated as following [30]:

$$x = \frac{l - v(t_A - t_B)}{2} \quad \text{……(2.3.5)}$$

Theoretically, both voltage and current waveforms can be used to calculate the fault distance. However, in practice, the current waveform is preferred due to the fact that some of the buses in

the transmission network have lower impedances, thus the voltage waveform traveling surge is reduced [30].

The major drawbacks are that the method requires a lot of information to implement such as standard time reference at line terminals, precise wave traveling time. A lot of equipment are also needed in this method such as GPS transducer, appropriate communication channel and instrumentation transformers (for example CTs which can measure the current). Besides, the method needs abundant simulations and heavily depends on operating conditions. Even though the traveling wave method may not cooperate with PMUs due to the presence of those specialized equipment, but it has the highest accuracy with the maximum error of $300m$, even for long transmission lines [31]. From the accuracy point of view, this method can provide a good comparison to the Two-Stage fault location algorithm.

2.4 Summary

In this chapter, some classic fault location methods like One-terminal, Multi-Terminal (mainly Two-Terminal method and Three-Terminal methods) and the Traveling Wave method have been reviewed. Those methods are most basic ones in fault location detection and still being widely used in utilities or mentioned in publications. They all have their own advantages, however, each one has some certain limitations when it comes to operate within the limitations of a PMU only linear state estimator. One-terminal method highly depends on fault resistance which makes it unreliable and inaccurate when dealing with high fault resistance faults. The requirement of a certain number of PMUs to be placed in the network makes the multi-terminal methods also unpractical due to the budget issues. Due to the requirement of sophisticated equipment and intensive simulations, the traveling wave method has major disadvantage if we want to use PMU only linear state estimator. Therefore, an easy, faster, accurate, independent of fault types and fault

resistance fault location algorithm which uses only a limited number of PMUs in the meantime is much needed.

Chapter 3: Two-Stage Fault Location Algorithm Using PMU Voltage Measurements

3.1 Introduction

Various fault location algorithms have been proposed during the past few decades, such as One-Terminal method, Multi-Terminal method and Traveling Wave method which have been reviewed in chapter 2. They all have some advantages, as well as some certain disadvantages which limit their performance. For example, the fault location estimation error for One-Terminal method may go up as the fault resistance increases. Multi-Terminal methods are limited mainly by the high density of PMUs installation requirement in power transmission network. The Traveling Wave method is majorly limited by the requirements of high accuracy/standard equipment as well as the tedious simulations. In this chapter, the two-stage PMU-based fault location algorithm proposed by Q. Jiang [14] is introduced with its basic theory in section 3.2.1. The tests of this Two-Stage algorithm on several standard IEEE systems are presented in section 3.2.2. This algorithm uses the relative transfer impedance on any bus and it is attractive when deal with linear state estimator monitored system since it only requires a limited number of PMU voltage measurements from the network to calculate the fault distance. This does not mean the PMUs can be placed at random buses. Optimal PMU locations, as in the case of linear state estimators, are still required due to the budget concerns. However, PMU placement is not the focus in this thesis, [20, 21] and [33]-[36] give some great ideas of optimal PMU placement. This fault location algorithm consists of two stages. The first stage is to find the suspicious fault buses and can be used as a detection or trigger stage when utilize the input data from the linear state estimator. The second stage is to select all the lines which connected to the suspicious fault buses, search along each of those lines and finally obtain the correct fault line with an accurate fault distance.

3.2 Two-stage PMU-based Fault Location Algorithm

3.2.1 Basic Theory and Example

Only positive sequence network exists in all types of fault, thus this algorithm only analyze the positive sequence parameters. It is also an attractive feature for implementation since most linear state estimators and PMU measurements are limited to positive sequence network. Consider Figure 3.1, for an n-bus power transmission network, if a fault occurs at point F between bus i and bus j with a fault distance x from bus i (where $0 < x < 1$). An equivalent π model is used to represent the transmission line.

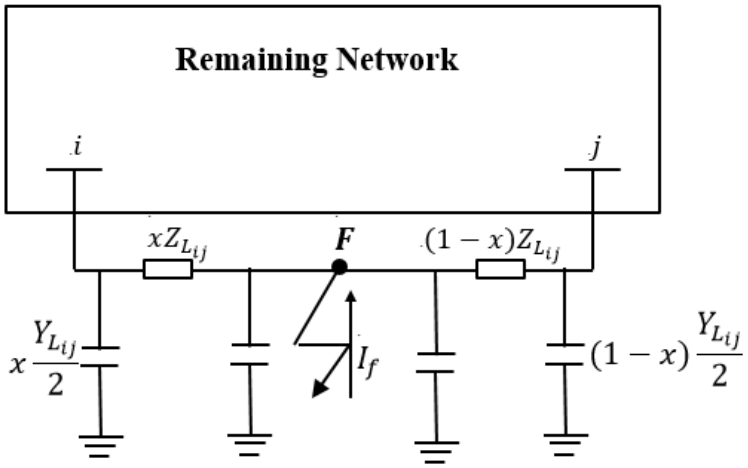

Figure 3. 1: Positive sequence network during the fault [14]. ([14] Q. Jiang, X. Li, B. Wang, and H. Wang, "PMU-based fault location using voltage measurements in large transmission networks," IEEE Trans. Power Del., vol. 27, no. 3, pp. 1644–1652, Jul. 2012. Used under fair use, 2015)

x: Fault distance from bus i

$Z_{L_{ij}}$: Equivalent line $(i-j)$ impedance

$Y_{L_{ij}}$: Equivalent line $(i-j)$ admittance

L_{ij}: Length of the line $(i-j)$

In [14], the authors did not mention how to obtain the pre- and post-fault system impedance matrices. Additional work are needed to obtain the correct matrices. Before the fault occurs, the

system admittance matrix Y^0 can be established in equation (3.2.1), with a dimension of $n \times n$. An important thing to mention is when construct this pre-fault admittance matrix Y^0, one must account for the generator admittance as well as the equivalent load admittance, instead of using only the transmission line parameters, otherwise it will completely change the final results and fail this algorithm.

$$Y^0 = \begin{bmatrix} Y_{11} & Y_{12} & \cdots & Y_{1n} \\ Y_{21} & Y_{22} & \cdots & Y_{2n} \\ \vdots & \vdots & \cdots & \vdots \\ Y_{n1} & Y_{n2} & \cdots & Y_{nn} \end{bmatrix} \quad \ldots\ldots(3.2.1)$$

From Figure 3.2, in post-fault period (it does not mean the fault has been cleared, the fault is still there), the fault point F provides a fault injection current I_f into the system, so it can be regarded as an additional bus. Now, the system has $n + 1$ buses, thus, the new system admittance matrix Y' has a dimension of $(n + 1) \times (n + 1)$ which is shown in equation (3.2.2).

$$Y' = \begin{bmatrix} Y_{11} & \cdots & Y_{1i} & \cdots & Y_{1j} & \cdots & Y_{1n} & 0 \\ \vdots & \cdots & \vdots & \cdots & \vdots & \cdots & \vdots & 0 \\ Y_{i1} & \cdots & Y'_{ii} & \cdots & Y'_{ij} & \cdots & Y_{in} & Y'_{i(n+1)} \\ \vdots & \cdots & \vdots & \cdots & \vdots & \cdots & \vdots & 0 \\ Y_{j1} & \cdots & Y'_{ji} & \cdots & Y'_{jj} & \cdots & Y_{jn} & Y'_{j(n+1)} \\ \vdots & \cdots & \vdots & \cdots & \vdots & \cdots & \vdots & 0 \\ Y_{n1} & \cdots & Y_{ni} & \cdots & Y_{nj} & \cdots & Y_{nn} & 0 \\ 0 & 0 & Y'_{(n+1)i} & 0 & Y'_{(n+1)j} & 0 & 0 & Y'_{(n+1)(n+1)} \end{bmatrix} \quad \ldots\ldots(3.2.2)$$

Since the fault point occurs only between bus i and bus j, the only 9 terms that will be changed are: Y'_{ii}, Y'_{ij}, Y'_{ji}, Y'_{jj}, $Y'_{i(n+1)}$, $Y'_{j(n+1)}$, $Y'_{(n+1)i}$, $Y'_{(n+1)j}$, $Y'_{(n+1)(n+1)}$. They can be derived from the original elements in pre-fault admittance matrix Y^0 based on equations (3.2.3) ~ (3.2.8),

$$Y'_{ii} = Y_{ii} - \frac{Y_{L_{ij}}}{2} - \frac{1}{Z_{L_{ij}}} + \frac{xY_{L_{ij}}}{2} + \frac{1}{xZ_{L_{ij}}} = Y_{ii} - \frac{(1-x)Y_{L_{ij}}}{2} - \frac{x-1}{xZ_{L_{ij}}} \quad \text{.....(3.2.3)}$$

$$Y'_{i(n+1)} = Y'_{(n+1)i} = -\frac{1}{xZ_{L_{ij}}} \quad \text{.....(3.2.4)}$$

$$Y'_{ij} = Y'_{ji} = Y_{ij} + \frac{1}{Z_{L_{ij}}} \quad \text{.....(3.2.5)}$$

$$Y'_{j(n+1)} = Y'_{(n+1)j} = -\frac{1}{(1-x)Z_{L_{ij}}} \quad \text{.....(3.2.6)}$$

$$Y'_{jj} = Y_{jj} - \frac{Y_{L_{ij}}}{2} - \frac{1}{Z_{L_{ij}}} + \frac{(1-x)Y_{L_{ij}}}{2} + \frac{1}{(1-x)Z_{L_{ij}}} = Y_{jj} - \frac{xY_{L_{ij}}}{2} - \frac{1}{Z_{L_{ij}}} + \frac{1}{(1-x)Z_{L_{ij}}} \quad \text{.....(3.2.7)}$$

$$Y'_{(n+1)(n+1)} = \frac{xY_{L_{ij}}}{2} + \frac{1}{xZ_{L_{ij}}} + \frac{(1-x)Y_{L_{ij}}}{2} + \frac{1}{(1-x)Z_{L_{ij}}} = \frac{Y_{L_{ij}}}{2} + \frac{1}{xZ_{L_{ij}}} + \frac{1}{(1-x)Z_{L_{ij}}} \quad \text{.....(3.2.8)}$$

In matrix Y', elements from row $(n+1)$ and column $(n+1)$ are all zeros other than the elements from (3.2.4), (3.2.6) and (3.2.8), and the remaining elements are exactly the same as elements in pre-fault matrix Y^0 except for the elements in (3.2.3), (3.2.5) and (3.2.7).

Among equations (3.2.3)-(3.2.8), the equivalent line impedance $Z_{L_{ij}}$ and equivalent line admittance $Y_{L_{ij}}$ are still unknown elements. However, since the equivalent π model is being analyzed in this algorithm, recall the transmission line representation models in section 2.1.1, those line model parameters from Figure 2.3 can be used to calculate $Z_{L_{ij}}$ and $Y_{L_{ij}}$:

$z_{ij} = series\ impedance\ per\ unit\ length\ for\ line\ i-j\ (\Omega/mile\ or\ \Omega/km)$
$y_{ij} = shunt\ admittance\ per\ unit\ length\ for\ line\ i-j\ (mho/mile\ or\ mho/km)$
$l_{ij} = length\ of\ line\ i-j\ (mile\ or\ km)$
$Z_{ij} = z_{ij}l_{ij} = total\ series\ impedance\ per\ phase\ for\ line\ i-j$
$Y_{ij} = y_{ij}l_{ij} = total\ shunt\ admittance\ per\ phase\ to\ neutral\ for\ line\ i-j$

$$Z_{c,ij} = characteristic\ impedance\ of\ line\ i-j = \sqrt{z_{ij}/y_{ij}}$$

$$\gamma = propagation\ constant = \sqrt{z_{ij}y_{ij}}$$

$$Z_{L_{ij}} = Z_{c,ij} \cdot \sinh(\gamma l_{ij}) = Z_{ij} \cdot \frac{\sinh(\gamma l_{ij})}{\gamma l_{ij}} \quad \text{……(3.2.9)}$$

$$Y_{L_{ij}} = \frac{\tanh\left(\frac{\gamma l_{ij}}{2}\right)}{Z_{c,ij}} = Y_{ij} \cdot \frac{\tanh\left(\frac{\gamma l_{ij}}{2}\right)}{\frac{\gamma l_{ij}}{2}} \quad \text{……(3.2.10)}$$

During fault, due to the presence of the injection fault current I_f, the nodal equation can be derived in equation (3.2.11),

$$\begin{bmatrix} \Delta V_1 \\ \vdots \\ \Delta V_i \\ \vdots \\ \Delta V_n \\ \Delta V_{n+1} \end{bmatrix} = Z' \begin{bmatrix} 0 \\ \vdots \\ 0 \\ \vdots \\ 0 \\ I_f \end{bmatrix} \quad \text{……(3.2.11)}$$

Where $Z' = (Y')^{-1}$, and ΔV_i is the voltage difference at bus i between pre-fault positive sequence voltage and post-fault positive sequence voltage* at that bus. Since most modified elements in matrix Y' are directly related to fault distance x, after taking the inverse of Y', every single element in matrix Z' will be related to fault distance x. Therefore, the post-fault system impedance matrix Z' has the form in equation (3.2.13).

$$\Delta V = \Delta V_{post}^{+} - \Delta V_{pre}^{+} \quad \text{……(3.2.12)}$$

$$Z' = \begin{bmatrix} Z_{11}(x) & Z_{12}(x) & \cdots & Z_{1n}(x) & Z_{1(n+1)}(x) \\ Z_{21}(x) & Z_{22}(x) & \cdots & Z_{2n}(x) & Z_{2(n+1)}(x) \\ \vdots & \vdots & \cdots & \vdots & \vdots \\ Z_{n1}(x) & Z_{n2}(x) & \cdots & Z_{nn}(x) & Z_{n(n+1)}(x) \\ Z_{(n+1)1}(x) & Z_{(n+1)2}(x) & \cdots & Z_{(n+1)n}(x) & Z_{(n+1)(n+1)}(x) \end{bmatrix} \quad \ldots\ldots(3.2.13)$$

Post-fault positive sequence voltage*: Post-post here does not mean the fault has been cleared, the fault is still there, and a stabilized (not the transient) fault bus voltage is obtained from PSS/E

From (3.2.11) and (3.2.13), the following equation can be obtained.

$$\Delta V_i = Z_{i(n+1)}(x) \cdot I_f \quad \ldots\ldots(3.2.14)$$

$$I_f = \frac{\Delta V_i}{Z_{i(n+1)}(x)} \quad \ldots\ldots(3.2.15)$$

Equation (3.2.15) illustrates that the fault injection current I_f can be represented by the voltage change on any bus and its relative transfer impedance, furthermore, this equation should be valid on any bus in the network. Thus, if two PMUs are placed at bus p and bus q in the network, the fault distance x can be solved by the following equation,

$$\frac{\Delta V_p}{Z_{p(n+1)}(x)} = \frac{\Delta V_q}{Z_{q(n+1)}(x)} \quad \ldots\ldots(3.2.16)$$

Assume m $(m \geq 2)$ PMUs are being placed in the network, when a fault occurs, the voltage difference ΔV_i can be obtained, where i represents the bus with a PMU is placed $(i = 1, 2, \cdots, m)$. The following equations can be defined,

$$K_i(x) = |I_f| = \left|\frac{\Delta V_i}{Z_{i(n+1)}(x)}\right| \quad (0 < x < 1) \quad \ldots\ldots(3.2.17)$$

From (3.2.17), it is easy to see that the term $K_i(x)$ is a function of fault distance x, furthermore, it only depends on the voltage change and transfer impedance. Therefore, it will not be affected by

the fault type and fault resistance. When combine (3.2.16) and (3.2.17), the following equation can be obtained,

$$K_1(x) = K_2(x) = \cdots = K_m(x) \quad \text{……(3.2.18)}$$

Ideally, the fault distance x can be calculated by the equation (3.2.18). However, it is hard to achieve in practice due to equation (3.2.18) is usually a non-linear and complex equation. The errors from PMU measurement and calculations make it impossible for all $K_i(x)$ to be exactly equal. To overcome this difficulty, a matching degree δ, is defined to simplify the problem.

$$\delta_i(x) = \sqrt{\frac{1}{m}\sum_{i=1}^{m}[K_i(x) - \overline{K}(x)]^2} \quad \text{……(3.2.19)}$$

$$\overline{K}(x) = \frac{1}{m}\sum_{i=1}^{m} K_i(x) \quad \text{……(3.2.20)}$$

This matching degree δ is also a function of fault distance x, and theoretically, if and only if at the exact fault point, $\delta = 0$. But in reality, this may not be true since the errors that involved in measurements as well as the calculations. Therefore, this fault location becomes to an optimization problem which is to find the minimum value for $\delta(x)$. In other words, the matching degree δ is minimum only at the fault point and the closer to the fault, the smaller the δ values will be. This claim is the backbone of the whole algorithm, and it is verified by two simple examples in Appendix I (a) and I (b).

- **Stage 1: Shrink Fault Location Searching Area**

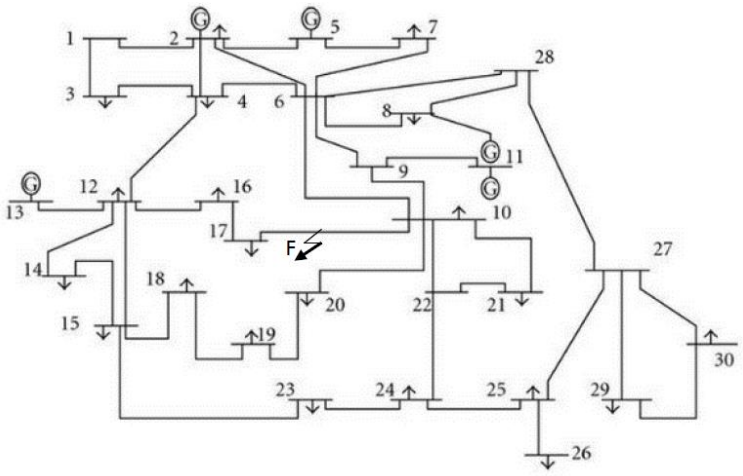

Figure 3. 2: 30-bus system with three-phase fault on line 10-17.

When a fault occurs in a large transmission network, it is tedious to search each transmission line in the network. Thus, minimize the searching area is necessary. Consider a 30-bus system with a three-phase fault between bus 10 and bus 17 shown in Figure 3.2.

When fault occurs at F, theoretically, the matching degree δ at point F is zero. And based on the topology of the system, bus 10 and bus 17 are the closest buses to the fault point, thus, the matching degree δ at bus 10 and bus $_{F}$ 17 should be close to zero. Furthermore, buses like 29 and 30 will have a relatively larger δ values compare to buses 10 and 17. So, the basic logic of stage 1 is: buses that are closer to the fault point, will have smaller δ values, and vice versa. However, this is not always true, it really depends on the topology of the system. A counter example along with the reason behind it will be presented later in this chapter.

To find the suspicious fault buses, it is necessary to calculate the δ values for all buses in order to find the minimum δ value, the corresponding bus can be regarded as the suspicious fault bus. To ensure the accuracy of the algorithm, it is necessary to pick several buses that have relatively smaller δ values as the suspicious fault buses instead of just single one bus with the minimum δ.

The pre-fault system bus impedance Z^0 must be used to calculate δ values for all the buses in Stage 1. For example, m PMUs being placed optimally in the network, and assume the fault occurs at bus 10 in Figure 3.2, the following equation can be derived,

$$K_i = \left|\frac{\Delta V_i}{Z^0_{i,10}}\right| \quad (i = 1, 2, \dots, m) \qquad \text{……(3.2.21)}$$

where i represents the bus where a PMU is placed, and $Z^0_{i,10}$ represents $(i, 10)^{\text{th}}$ element in pre-fault system impedance matrix Z^0. It can be seen that equation (3.2.21) and equation (3.2.17) are similar, the only different is (3.2.21) uses the pre-fault impedance while (3.2.17) uses the post-fault impedance which contains the function of fault location information x. From (3.2.19) and (3.2.21), if a fault occurs at bus 10, the matching degree δ_{10} can be obtained,

$$\delta_{10} = \sqrt{\frac{1}{m}\sum_{i=1}^{m}[K_i - \overline{K}]^2} \qquad \text{……(3.2.22)}$$

where, $\overline{K} = \frac{1}{m}\sum_{i=1}^{m} K_i$. Usually, not all the PMU measurements are selected. Due to the fact that under large fault resistance condition, the voltage change at some buses may not be significant, thus leads to an inaccurate fault location estimation. Therefore, only partial PMU measurements that have a larger voltage change will be selected.

The detailed procedure of Stage 1 can be summarized as following:

1) Establish the pre-fault system impedance matrix Z^0.
2) Obtain m PMU voltage measurements before and after the fault (to calculate the voltage change ΔV).
3) Select only n $(n \leq m)$ PMU voltage measurements that give relatively large voltage changes.

4) Calculate the matching degrees δ_i at all buses, where $i = 1, 2, \dots, n$ by using (3.2.21)
5) Select several buses that have relatively smaller δ values as the suspicious fault buses, and regard the lines connected to those buses as suspicious fault lines.

The flowchart of Stage 1 is shown in Figure 3.3,

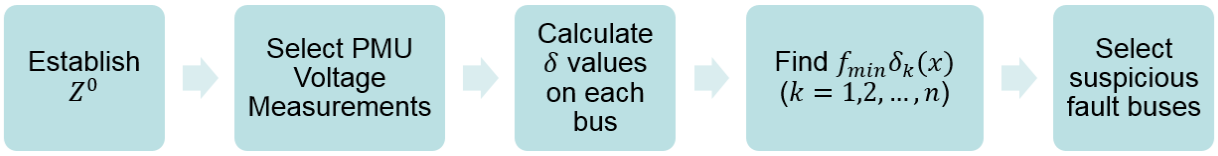

Figure 3. 3: Flow chart of Stage 1: Narrow down the searching area.

- **Stage 2: Find Exact Fault Point**

Once the searching area has been narrowed down and the suspicious buses have been identified, next step is to search along those possible fault lines which connected to those suspicious fault buses in order to find the exact fault point. The updated post-fault system impedance matrix Z' must be used in Stage 2. The detailed procedure is summarized,

1) N lines $(L_1, L_2, \dots, L_N)$ have been selected from Stage 1 as the suspicious fault lines.
2) Search along the line L_i (where $i = 1, 2, \dots, N$) by a small step change Δx (Δx is set to 0.0001 in this thesis), and obtain the $\delta(x)$ values for each new $x = k \cdot \Delta x$ (where $k = 1, 2, \dots, 1/\Delta x$) by using equation (3.2.17).
3) Find the minimum $\delta(x)$ value in the whole data set of $\{L_i, x_i\}$
4) The fault line L_i as well as the fault distance x that correspond to the minimum $\delta(x)$ value is the estimated fault point at the estimated fault line.

The flowchart of stage 2 is shown in Figure 3.4 below,

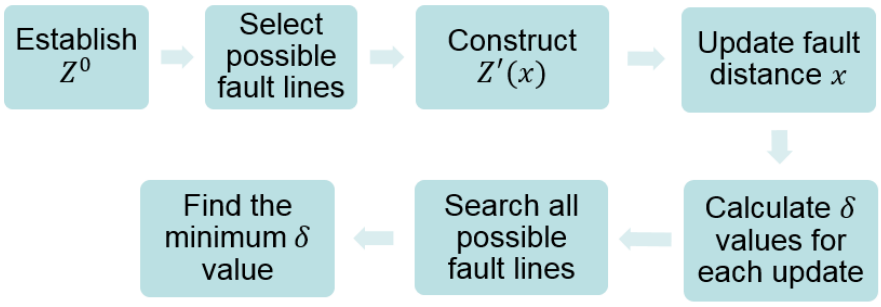

Figure 3. 4: Flow chart of Stage 2: Find the exact fault location.

3.2.2 Implementation of the Two-Stage fault location algorithm on IEEE 9-bus systems

In previous section, the basic theory and derivation of the Two-stage fault location algorithm have been presented. In this section, the testing on IEEE 9-bus system (shown in Figure 3.5) is performed. The system parameter is shown in Appendix II. Assume 3 PMUs are placed at generator buses 1, 2 and 3.

When implementing the algorithm, a PSS/E model must be built first. The "Solve and report network with unbalances" function in PSS/E can perform the fault analysis. In this function, users can select different fault types, different fault impedances and set their own fault distance on any transmission line under the "In line slider" tab. The post-fault voltages at each bus can be obtained from the output report. The positive sequence voltage difference ΔV_i on PMU-located buses can be calculated. Once ΔV_i , Z^0 and Z' are obtained, the actual algorithm can be implemented in Matlab.

- **Implement the algorithm on IEEE 9-bus system and verify the stage 1**

Consider the IEEE 9-bus test system shown in Figure 3.5. All lines (totally 9) need to be tested for different fault types and different fault resistance which is shown in Table 1 below.

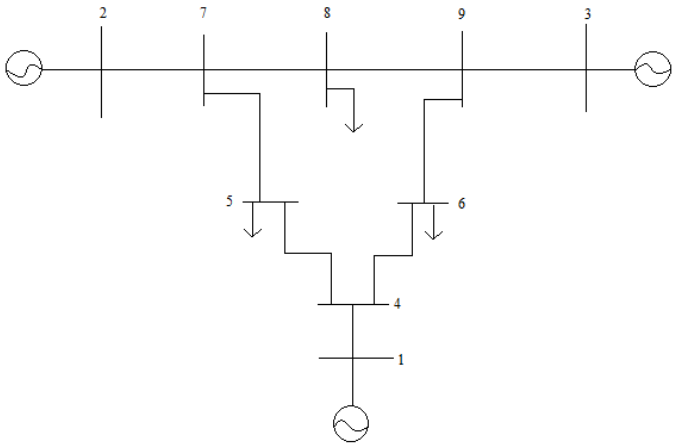

Figure 3. 5: IEEE 9-bus system with 3 PMUs at bus 1, 2 and 3.

Line to be tested	Fault Type	Fault Resistance (Ω)	Simulated Fault Location
1-4	AG	1	43% from 1
2-7	$3-\Phi$	-	56% from 2
3-9	$3-\Phi$	-	75% from 3
4-5	ABG	5	23% from 4
4-6	ACG	50	67% from 4
5-7	BCG	200	82% from 5
6-9	AG	50	73% from 6
7-8	ABG	100	16% from 7
8-9	BG	1000	61% from 8

Table 1: Implementation cases for IEEE 9-bus system

Based on Stage 1 of the algorithm, under each fault condition, the matching degree δ at every bus have been calculated and plotted in Figure 3.6 ~ Figure 3.14,

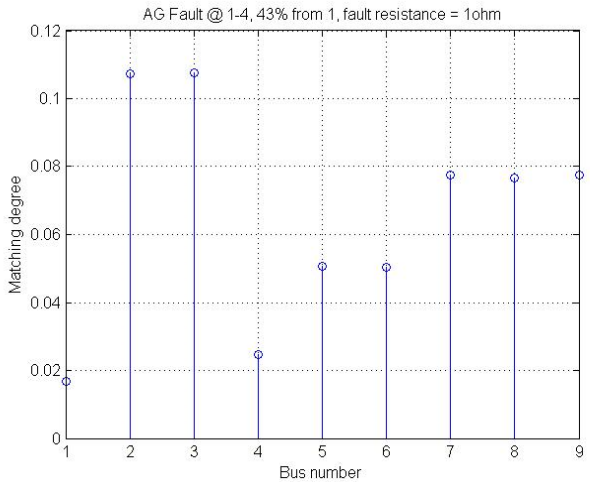

Figure 3. 6: Matching degree values for all buses with AG fault on line 1-4, 43% from bus 1, R_f=1Ω.

From Figure 3.6, it can be seen that bus 1 has the minimum matching degree δ_1, which successfully indicates that the suspicious fault bus is bus 1. Furthermore, it can be observed that the fault is closer to bus 1 than bus 4, this also successfully verified that the aforementioned claim that the closer to the fault point the smaller the matching degree δ will be. Ideally, the minimum two δ values should be observed and it will directly tell us that the fault is on the line between those two corresponding buses. Like in Figure 3.6, δ_1 and δ_4 are the two minimum values, which indicates that the fault is most likely on the line between bus 1 and bus 4. However, to ensure the accuracy and reliability, usually, several relatively smaller δ values should be selected, and their corresponding buses should be regarded as the suspicious fault buses.

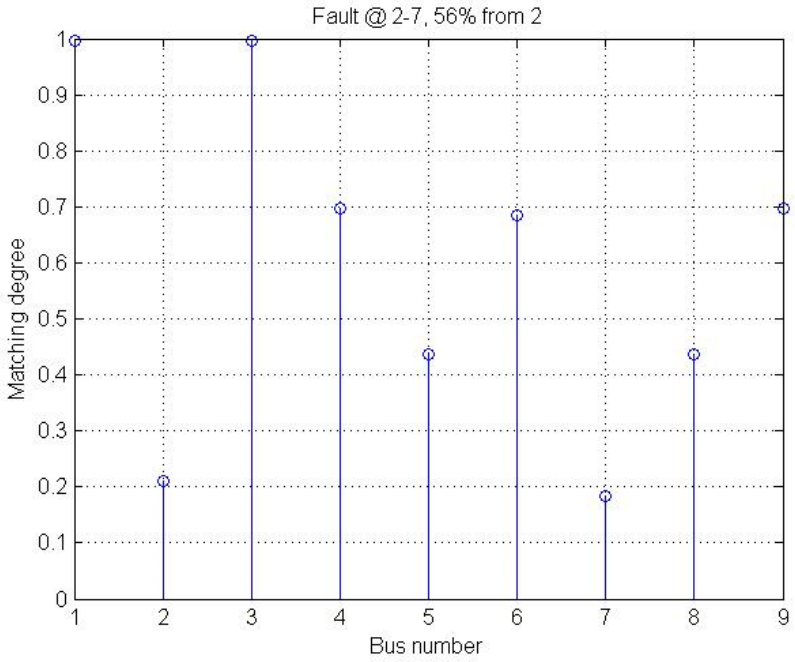

Figure 3. 7: Matching degree for all buses when three-phase fault is on line 2-7, 56% from bus 2.

Based on Figure 3.7, it can be observed that δ_2 and δ_7 are significantly smaller than any other bus in the system, which indicates that the most suspicious fault buses are 2 and 7, and most likely the fault is on line 2-7. Since there is no distinct difference between δ_2 and δ_7, it is unclear

which bus that the fault is closer to. The assumption could be the fault is in the middle section of the line, and Stage 2 is needed to verify this assumption.

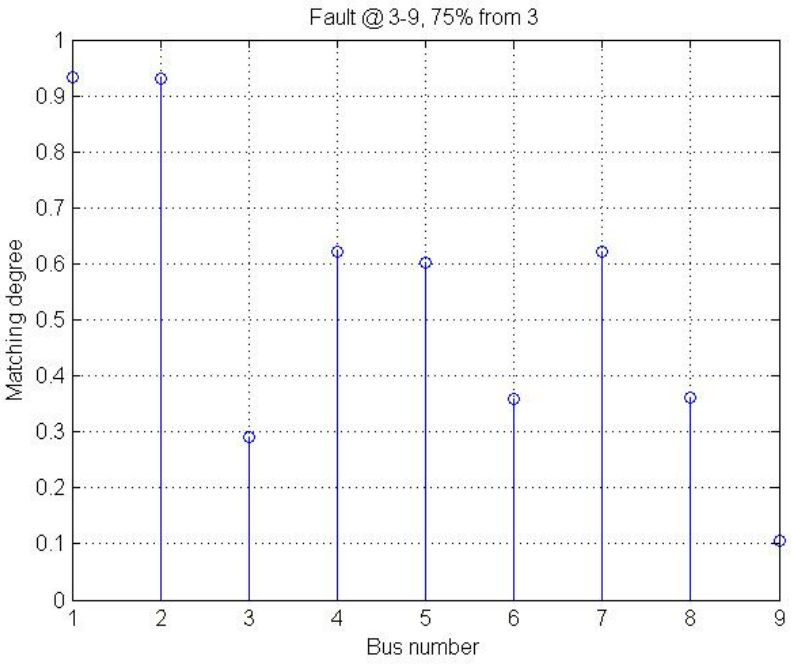

Figure 3. 8: Matching degree for all buses when three-phase fault is on line 3-9, 75% from bus 3.

From Figure 3.8, it is easy to see that δ values for bus 3 and 9 (δ_3 and δ_9) are smaller than other buses, which indicates that the most suspicious fault buses are bus 3 and 9, and most likely the fault is on the line 3-9. Refer to Figure 3.5, bus 6 and bus 8 are also connected with bus 9, so when the fault occurs, those two buses also have a relatively small δ values. To ensure the accuracy, bus 6 and 8 should also be selected as the fault buses. Furthermore, since δ_9 is much smaller than δ_3, the assumption that the fault is closer to bus 9 rather than bus 3 can be made. And this assumption does match the fault simulation condition, however, it still needs to be verified by Stage 2.

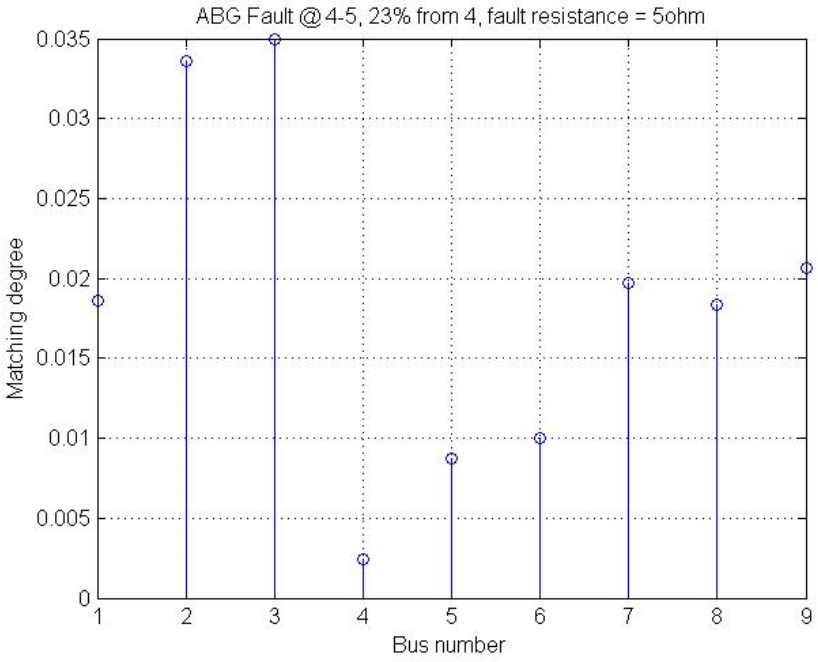

Figure 3. 9: Matching degree for all buses when ABG fault is on line 4-5, 23% from bus 4, R_f=5Ω.

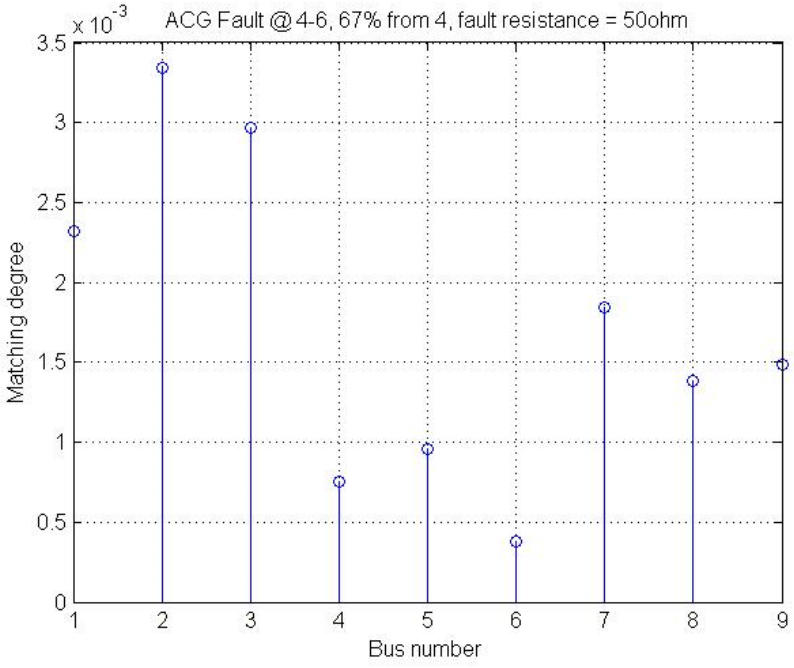

Figure 3. 10: Matching degree for all buses when ACG fault is on line 4-6, 67% from bus 4, R_f=50Ω.

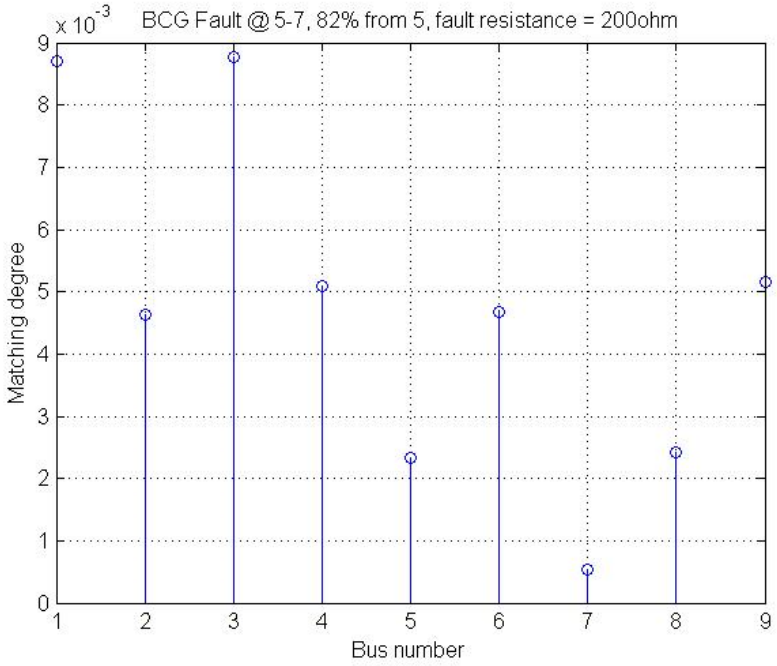

Figure 3. 11: Matching degree for all buses when BCG fault is on line 5-7, 82% from bus 5, R_f=200Ω.

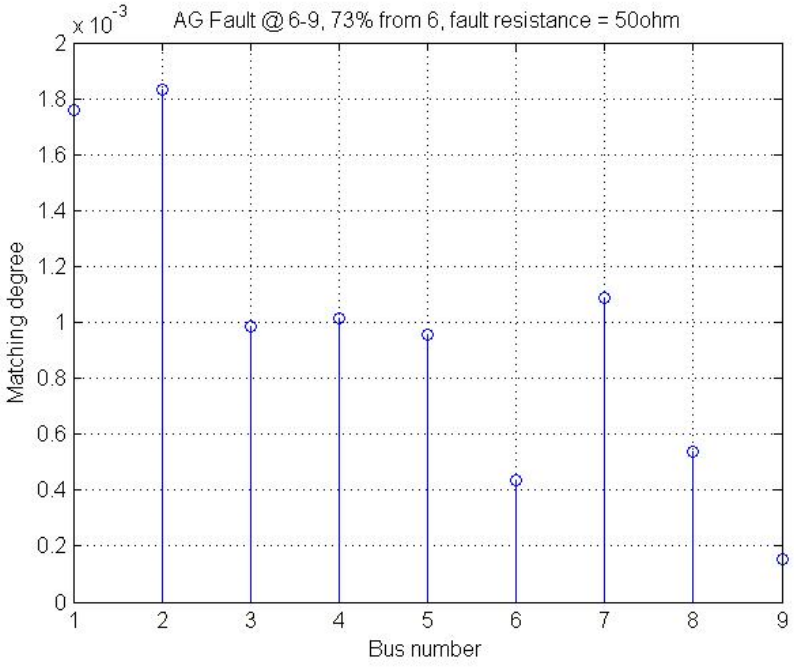

Figure 3. 12: Matching degree for all buses when AG fault is on line 6-9, 73% from bus 6, R_f=50Ω.

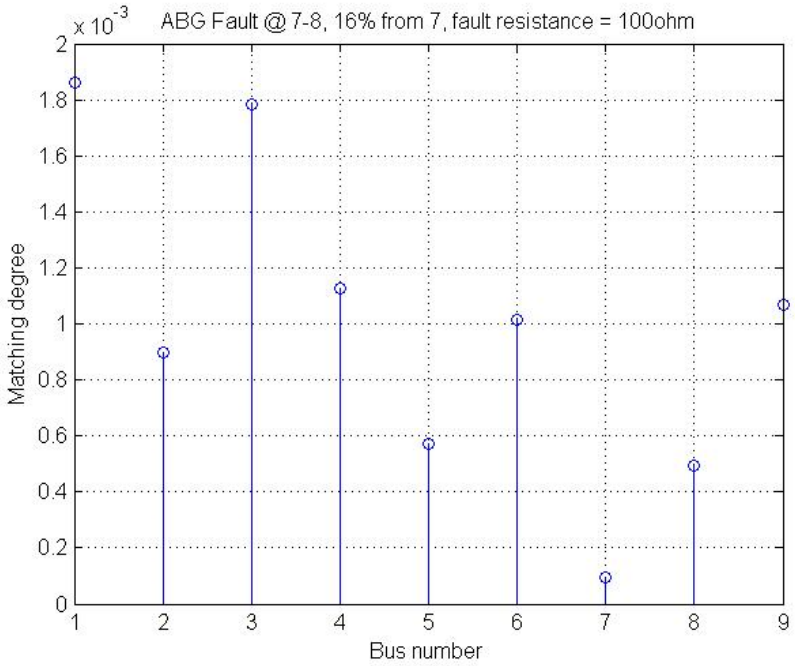

Figure 3. 13: Matching degree for all buses when ABG fault is on line 7-8, 16% from bus 7, R_f= 100Ω.

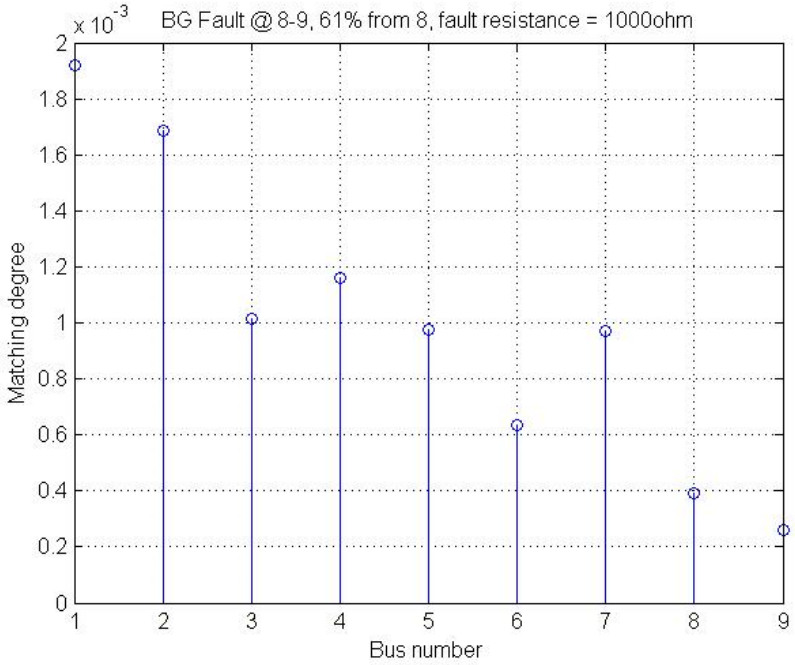

Figure 3. 14: Matching degree for all buses when BG fault is on line 8-9, 61% from bus 8, R_f= 1000Ω.

Figures 3.9~3.14 also show that the algorithm has been successfully implemented on IEEE 9-bus system for Stage 1. Now, all the lines in the system have been tested, and the results have shown that the Stage 1 is legit. Once the fault searching area has been narrowed down and the suspicious fault buses have been identified, it is relatively easy to locate the exact fault point.

- **Implement the algorithm on IEEE 9-bus system and verify the stage 2**

Table 2 below shows the fault location testing results for Stage 2 under only three-phase fault condition since it is the most severe fault type. And define the percentage of the estimated fault location error as the following:

$$Fault\ Location\ Error(\varepsilon) = \frac{|Estimated\ distance - Actual\ distance|}{Line\ length} \times 100\% \qquad \ldots\ldots(3.2.23)$$

All the lines are assumed to be 1p.u length.

Tested Lines	Actual Fault Locations	Able to Find Suspicious Buses?	Estimated Fault Locations	Minimum Matching Degree δ	Fault Location Error (ε)
1-4	85% from 1	Yes	85.11% from 1	0.0056	0.11%
2-7	56% from 2	Yes	56.00% from 2	1.0474e-4	0.00%
3-9	75% from 3	Yes	75.13% from 3	0.0073	0.13%
4-5	35% from 4	Yes	35.10% from 4	0.0051	0.10%
4-6	20% from 4	Yes	20.08% from 4	0.0049	0.08%
5-7	67% from 5	Yes	66.96% from 5	0.0052	0.04%
6-9	5% from 6	Yes	5.17% from 6	0.0051	0.17%
7-8	13% from 7	Yes	13.14% from 7	0.0058	0.14%
8-9	27% from 8	Yes	27.05% from 8	0.0049	0.05%

Table 2: IEEE 9-bus system fault location testing results for only three-phase fault.

From Table 2, it can be seen that the maximum error is 0.17%. So, if the transmission line is 100 km long, the accuracy would be 170 m. If the calculation errors can be eliminated, the fault location error should be less than 0.17%.

However, three-phase fault is not the only fault type, and usually, it is not most common fault as well. Therefore, other types of faults (such as L-G, L-L-G) must be tested. The testing results for Stage 1 Stage 2 are shown in Table 3,

Tested Lines	**Fault Type**	**Actual Fault Locations**	**Fault Resistance** (Ω)	**Able to Find Suspicious Buses?**	**Estimated Fault Locations**	**Minimum Matching Degree δ**	**Fault Location Error (ε)**
1-4	AG	43% from 1	1	Yes	43.02% from 1	7.8198e-04	0.02%
2-7	BG	38% from 2	10	Yes	38.05% from 2	8.3808e-05	0.05%
3-9	CG	87% from 3	100	Yes	87.08% from 3	1.7983e-04	0.08%
4-5	ABG	23% from 4	5	Yes	23% from 4	1.9476e-04	0.00%
4-6	ACG	67% from 4	50	Yes	67.06% from 4	7.3917e-05	0.06%
5-7	BCG	82% from 5	200	Yes	82.11% from 5	2.2197e-04	0.11%
6-9	AG	73% from 6	50	Yes	73.03% from 6	9.1170e-06	0.03%
7-8	ABG	16% from 7	100	Yes	15.93% from 7	3.8666e-05	0.07%
8-9	BG	61% from 8	1000	Yes	61.13% from 8	1.2402e-04	0.13%

Table 3: IEEE 9-bus system fault location testing results for other types of faults.

For different types of faults and fault resistance, the testing results showed that all the suspicious fault buses are successfully identified (Stage 1 verified) and the fault distance are also being estimated with a maximum error of 0.13%. Based on the testing results from both Table 1 and Table 2, this Two-stage fault location algorithm has been verified. Table 2 is also able to show that the algorithm is not affected by the fault type and fault resistance.

3.2.3 Implementation of the Two-Stage fault location algorithm on IEEE 39-bus systems

- **Implement the algorithm on IEEE 39-bus system and verify the stage 1**

To further implement this algorithm, an IEEE 39-bus system [38] is being used. The system is more complex and should provide a good indication of how accurate this new fault location algorithm will be. The 39-bus system diagram is shown in Figure 3.15 and the system parameters are shown in Appendix III. Only 10 PMUs are installed in the system at buses 28 and 30~38 [14].

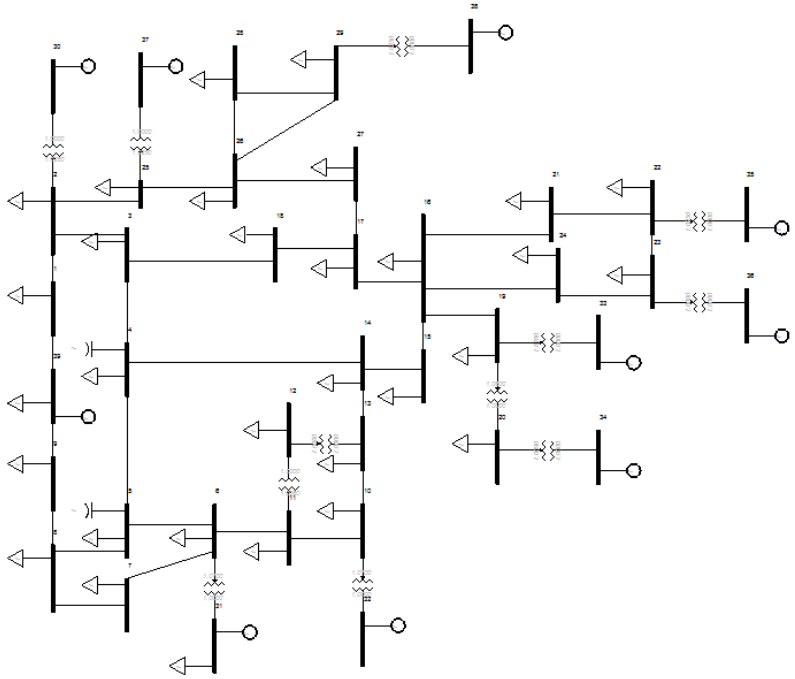

Figure 3. 15: One-line diagram of IEEE 39-bus system.

The Two-Stage fault location algorithm is implemented on all 34 transmission lines in the system for different fault types with different fault resistance. But only several representative tests are be shown in Table 4 and Figure 3.16~3.21.

Line To Be Tested	**Fault Type**	**Fault Resistance** (Ω)	**Simulated Fault Location**
3-18	Three-phase	-	15% from 3
4-14	Three-phase	-	70% from 4
5-8	ABG	50	65% from 5
6-11	ACG	200	10% from 6
14-15	BG	100	55% from 14
16-24	CG	500	40% from 16

Table 4: Implementation cases for IEEE 39-bus system

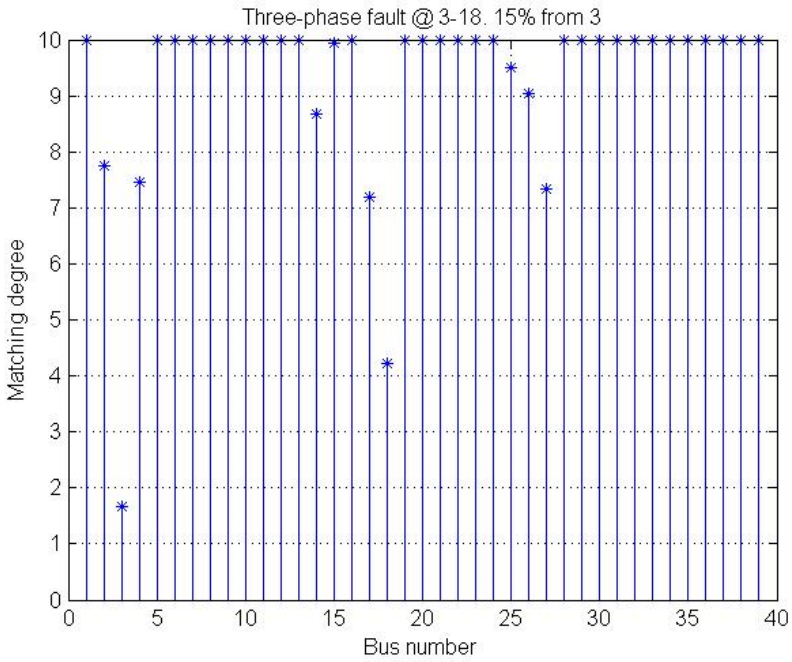

Figure 3. 16: Three-phase fault occurs on line 3-18, 15% from bus 3.

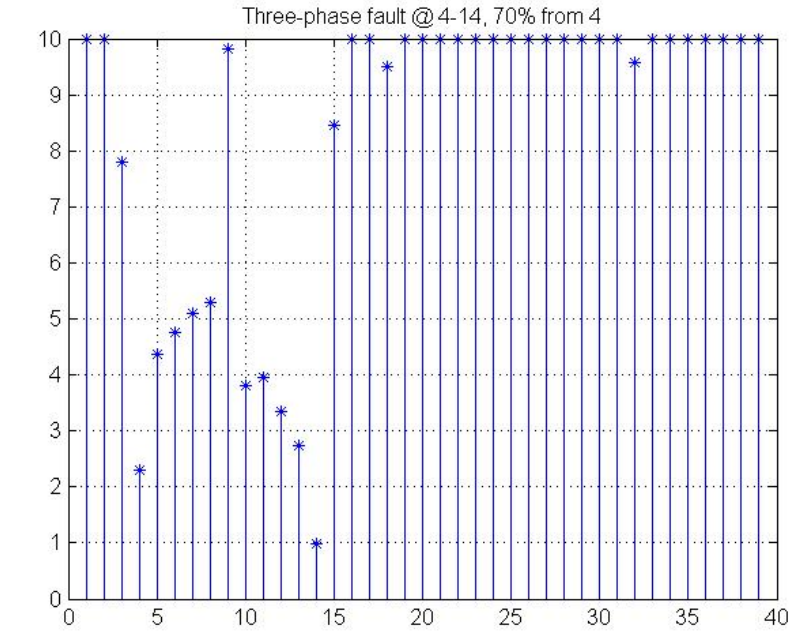

Figure 3. 17: Three-phase fault occurs on line 4-14, 70% from bus 4.

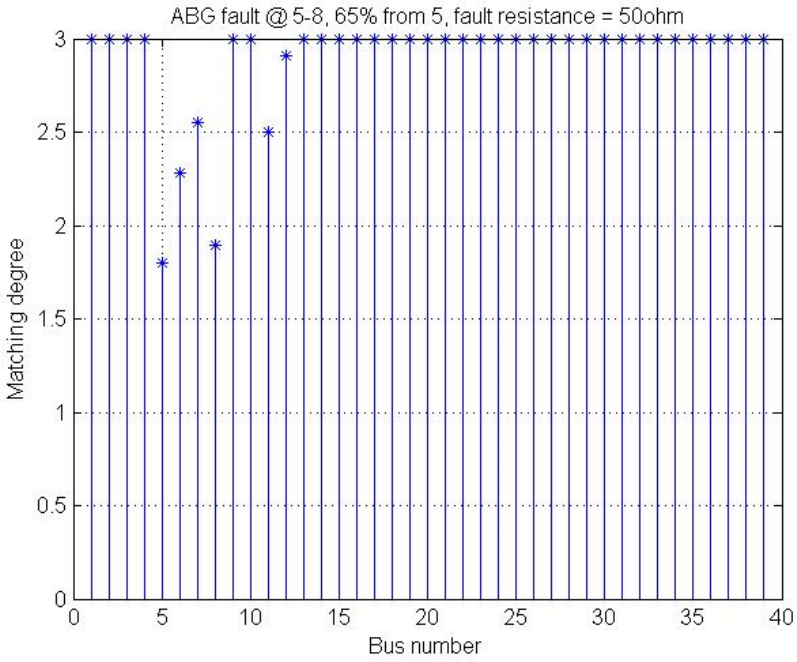

Figure 3. 18: ABG fault on line 5-8, 65% from bus 5, R_f=50Ω.

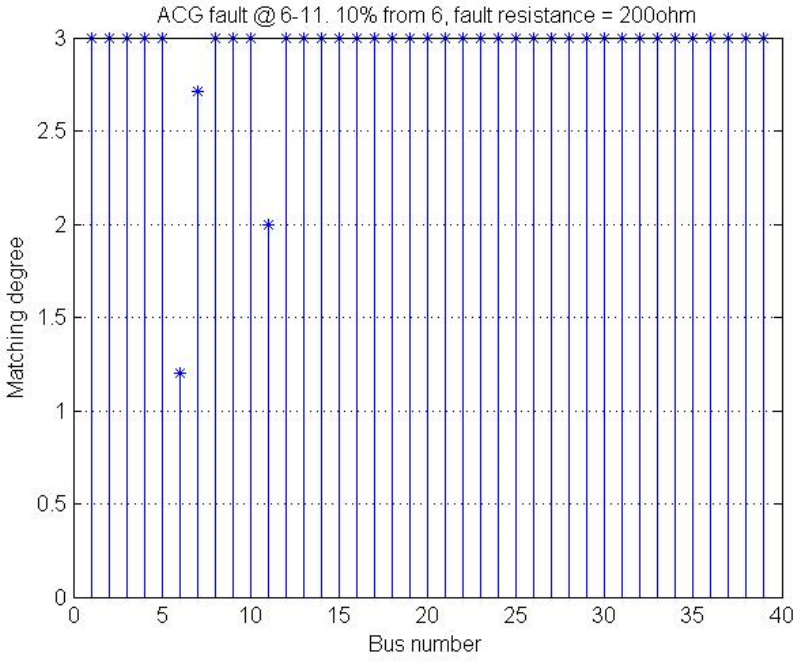

Figure 3. 19: ACG fault on line 6-11, 10% from bus 6, R_f=200Ω.

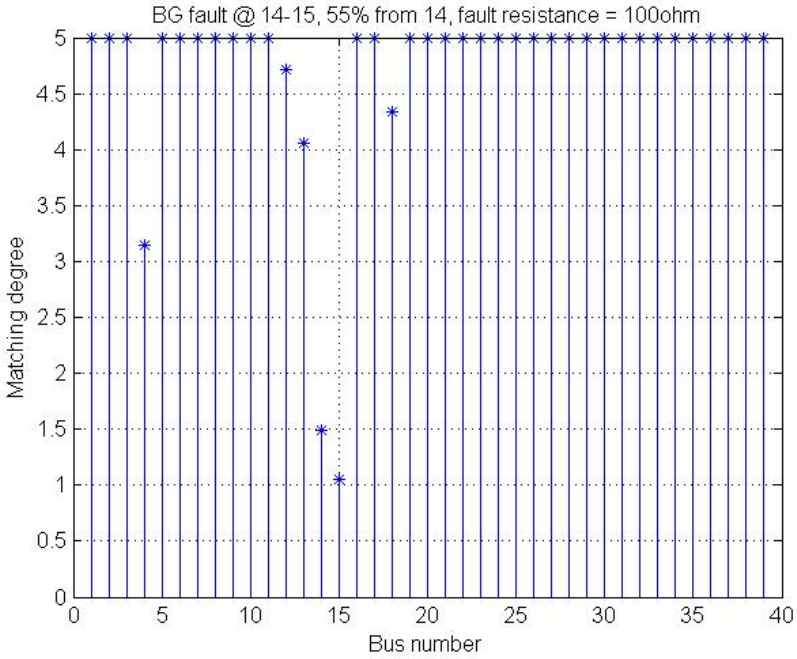

Figure 3. 20: BG fault on line 14-15, 55% from bus 14, R_f= 100Ω.

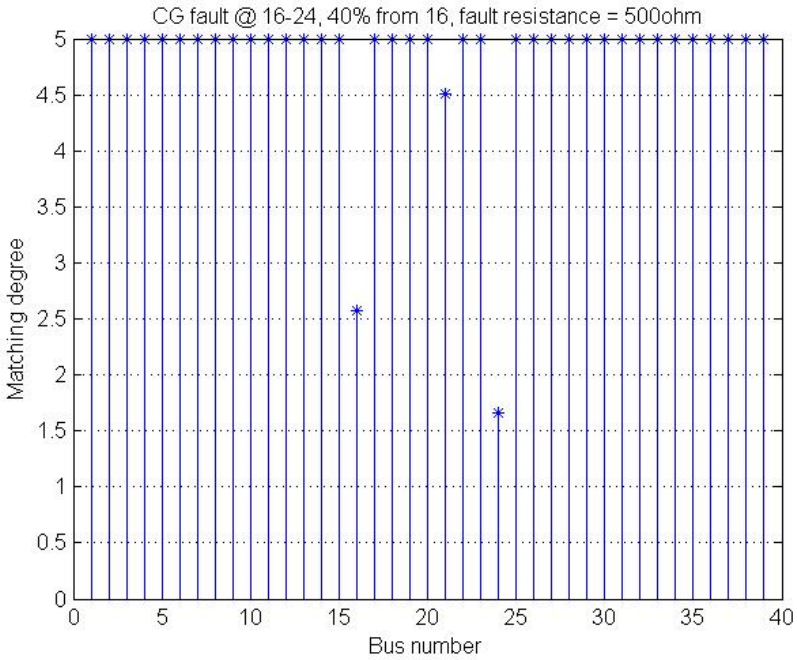

Figure 3. 21: CG fault on line 16-24, 40% from bus 16, R_f= 500Ω.

Noticed that in Figures 3.16~3.21, the matching degree δ values are set to 10 or 5 when they exceed 10 or 5 respectively. All testing plots could identify all the suspicious fault buses for different fault locations. Additionally, for most of the cases the algorithm is able to show that the faulted line is actually connected by the two suspicious fault buses, and the closer to the fault, the smaller the δ value will be. However, in some cases, it is not always true that the closer to the fault, the smaller the δ value. Refer to Figure 3.21, the fault is closer to bus 16, but δ_{16} has a larger value than δ_{24}. The reason is related to the system topology. If the two suspicious fault buses both have few transmission lines connected to them respectively, when a fault occurs, the voltages on those two buses will drop accordingly with fault distance. But if one of the buses has many transmission lines connected to it, when a fault occurs, the voltage drop on that bus may not be significant. This will affect the PMU voltage measurements (causes smaller voltage drop) near that bus. When it comes to calculate K_i, some outliers may show up due to the low voltage changes at some PMU buses. Those outliers cannot be ignored since they represent the system topology. Recall that the matching degree δ is the standard deviation of all the K_i values, therefore, with the presence of few outliers in K_i, δ value will be larger.

Refer to Figure 3.15, bus 16 has the most number of transmission lines (totally 5) in the system connected to it while bus 24 only has 2 transmission lines connected to it. This explains that even though the fault is closer to bus 16, but δ_{16} still larger than δ_{24}.

- **Implement the algorithm on IEEE 39-bus system and verify the stage 2**

Tested Lines	Fault Type	Actual Fault Locations	Fault Resistance (Ω)	Able to Find Suspicious Fault Buses?	Estimated Fault Locations	Fault Location Error
3-18	Three-phase	15% from 3	1	Yes	14.87% from 3	0.13%
4-14	Three-phase	70% from 4	5	Yes	70.21% from 4	0.21%
5-8	ABG	65% from 5	50	Yes	65.08% from 5	0.08%
6-11	ACG	10% from 6	200	Yes	9.73% from 6	0.27%
14-15	BG	55% from 14	100	Yes	55.11% from 14	0.11%
16-24	CG	40% from 16	500	Yes	40.17% from 16	0.17%

Table 5: IEEE 39-bus system fault location testing results for different fault types along with different fault resistance.

From Table 5, the estimated fault location results show that this algorithm has been successfully implemented on IEEE 39-bus system with only 10 PMUs being placed. This algorithm is also independent of fault types and fault resistance. The maximum fault location error is 0.39% which happens for the case of three-phase fault on line 17-18, 25% from 18. The accuracy of this algorithm is still acceptable.

3.3 Summary

In this chapter, the Two-stage fault location algorithm has been introduced. The basic theory is that a limited number of PMU voltage measurements, and the pre- and post-fault system equivalent impedance matrix are being utilized to calculate the matching degree δ. Usually, the closer to the fault point, the smaller the matching degree values δ will be. By using this claim, the first stage is to minimize the searching area by identifying several suspicious fault buses who have the relatively smaller δ values. The second stage is to find the exact fault location by searching all the lines connected to the suspicious fault buses. The most attractive part of this algorithm is that

it only requires a limited number of PMUs to be installed, this is extremely beneficial when it comes to deal with the linear state estimator monitored transmission system. Besides, this algorithm is not affected by the fault type and fault resistance. Based on the IEEE 9-bus system and IEEE 39-bus system case studies, it is easy to see that the algorithm has been successfully implemented without tedious calculations and simulations. It also gives a good fault location estimations as well.

The concept of this algorithm is based on the well-known transfer impedance. But the derivation of the pre-fault impedance requires additional work. Usually, the Y-bus matrix can be derived based on line parameters, and the exported Y-bus data from PSS/E uses exactly those line parameter data to construct the system admittance matrix. However, after testing the method by using this Y-bus matrix, it did not give the correct results for both stage 1 & 2. The equivalent load admittance as well as the generator admittance should be used and modeled correctly when building the pre-fault system admittance matrix.

To obtain the post-fault system impedance matrix Z', authors in [14] suggested that it can be done by directly modifying the corresponding elements in pre-fault system impedance matrix Z^0. This is not the correct way to do it. If the corresponding elements in Z^0 is modified based on where the fault is, there is no way that every element in Z' is related to fault distance x, thus the stage 2 cannot be achieved. The correct way is to modify the corresponding elements in pre-fault system admittance matrix Y^0, not directly in Z^0, to obtain the post-fault system admittance Y'. Most of the modified elements are related to the fault distance x, thus when inverting Y', every elements in Z' is related to the fault distance x.

Chapter 4: Algorithm Implementation on A Practical Transmission Network

4.1 Introduction

In previous chapter, the Two-Stage fault location algorithm has been successfully implemented on IEEE 9-bus and IEEE 39-bus systems. For a practical high voltage transmission network, the performance of this algorithm still remains to be evaluated. In this chapter, the Two-Stage fault location algorithm will be implemented on a practical 500kv 44-bus, PMU only linear state estimator monitored transmission network. The testing results for stage 1 & 2 are provided and evaluated.

4.2 Implementation of the Two-Stage fault location algorithm on a practical transmission network

Consider a practical 500kv 44-bus (numbered from 1 to 44) transmission network shown in figure 4.1 below.

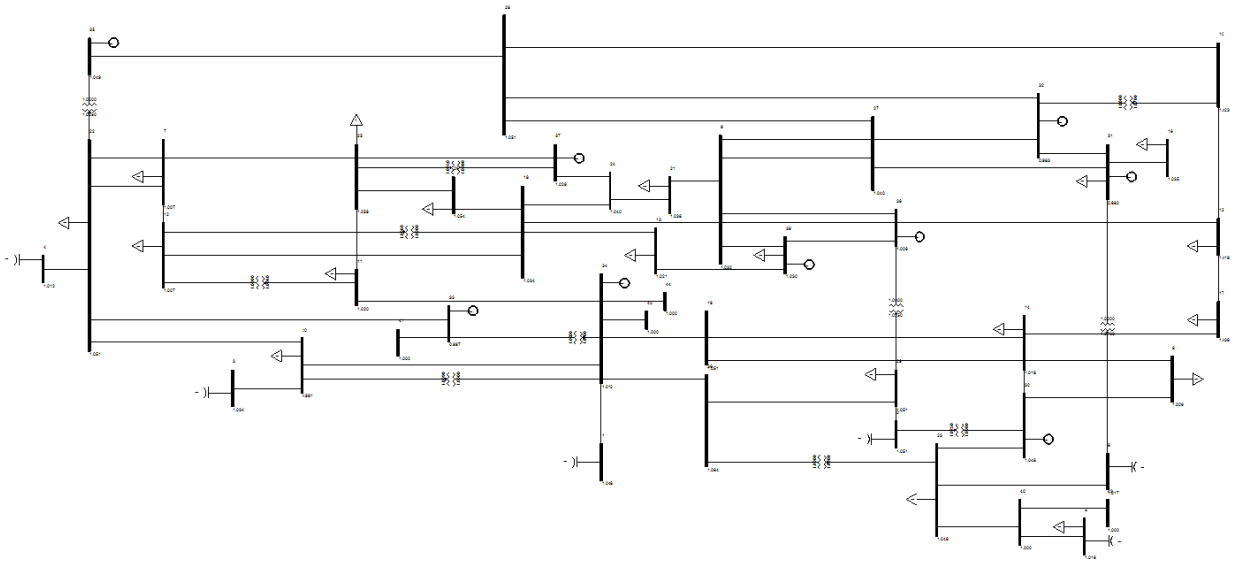

Figure 4. 1: A practical 500kv 44-bus transmission network.

In this practical system, 15 PMUs are placed at buses 7, 14, 18, 20, 22, 23, 24, 29, 29, 30, 31, 33, 34, 39 and 40 to provide the full observability of the system. Fault are placed on all lines to check the performance of the algorithm. A few representative cases of all 51 tested cases will be presented.

- **Implement the algorithm on the 44-bus system and verify the stage 1**

Sixteen cases were selected to demonstrate the effectiveness of the modified algorithm for different fault types and fault resistance as shown in Table 6 below.

Test #	Lines To Be Tested	Actual Fault Location	Fault type	Fault Impedance (p.u)
1	2-29	75% from 2	3 – Φ	-
2	9-27	47% from 9	3 – Φ	-
3	10-15	15% from 10	3 – Φ	-
4	11-25	23% from 11	3 – Φ	-
5	14-17	50% from 14	3 – Φ	-
6	16-31	10% from 31	3 – Φ	-
7	21-24	50% from 21	3 – Φ	-
8	38-39	66% from 38	3 – Φ	-
9	8-19	55% from 8	AG	1
10	8-19	55% from 8	AG	0.01
11	8-19	55% from 8	ABG	1
12	8-19	55% from 8	ABG	0.001
13	18-24	82% from 18	AG	0.1
14	18-24	82% from 18	AG	0.001
15	18-24	82% from 18	ACG	0.1
16	18-24	82% from 18	BCG	0.001

Table 6: Implementation cases for 44-bus system

Since three-phase fault is the most severe fault type, and usually, the voltage drop and fault current level will be large, it will account for the most difficult cases for the algorithm. Thus, more three-phase fault were tested. Tests 9 to16 demonstrate the performance under different fault types with different fault resistance. The main objective of stage 1 is to find the suspicious fault buses. Ideally, we should be able to directly identify the two suspicious fault buses where the fault occurs

between. The test results are shown on Figures 4.2 to 4.17. Each figure plots the computed matching degree for each of the 44 buses.

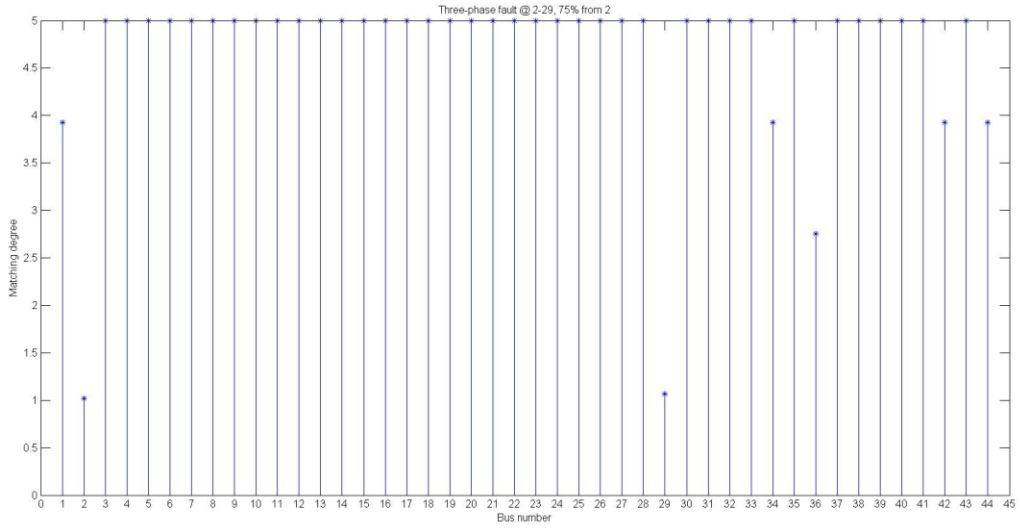

Figure 4. 2: Three-phase fault on line 2-29, 75% from 2.

From Figure 4.2, it is easy to see that bus 2 and bus 29 have the minimum two δ values, which implies that bus 2 and bus 29 are the suspicious fault buses, and most likely, the fault is between these two buses.

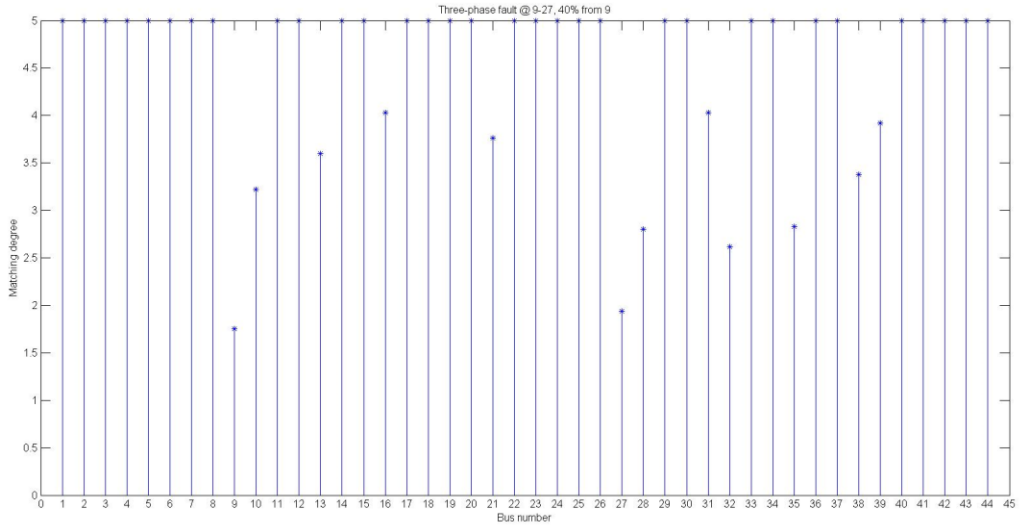

Figure 4. 3: Three-phase fault on line 9-27, 47% from 9.

Based on Figure 4.3, bus 9 and bus 27 have the two minimum δ values. So, those two buses are the suspicious fault buses.

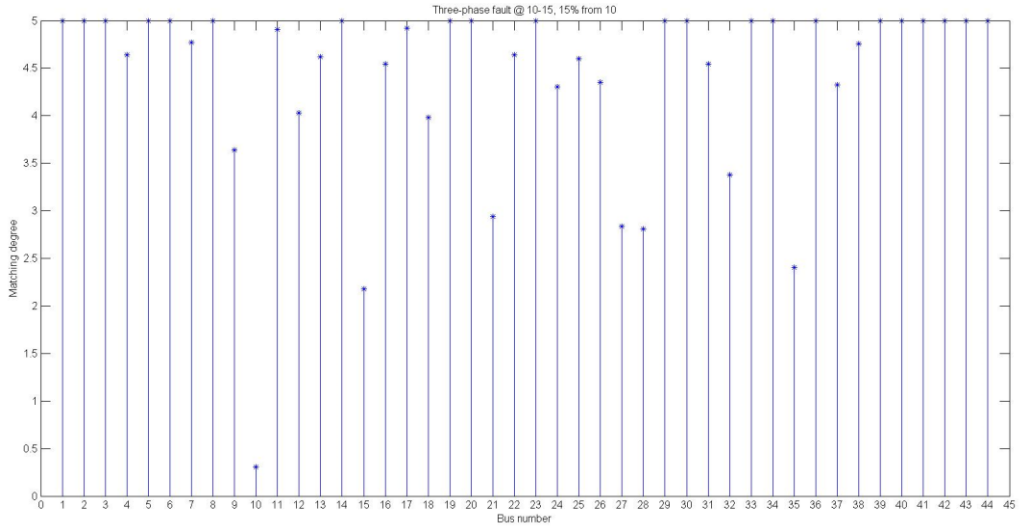

Figure 4. 4: Three-phase fault on line 10-15, 15% from 10.

From Figure 4.4, bus 10 and bus 15 have the two minimum δ values. And in this case, since the fault is much closer to bus 10, thus bus 10 has smaller delta values than bus 15, which also proves the aforementioned claim that "the closer to the fault, the smaller the δ will be".

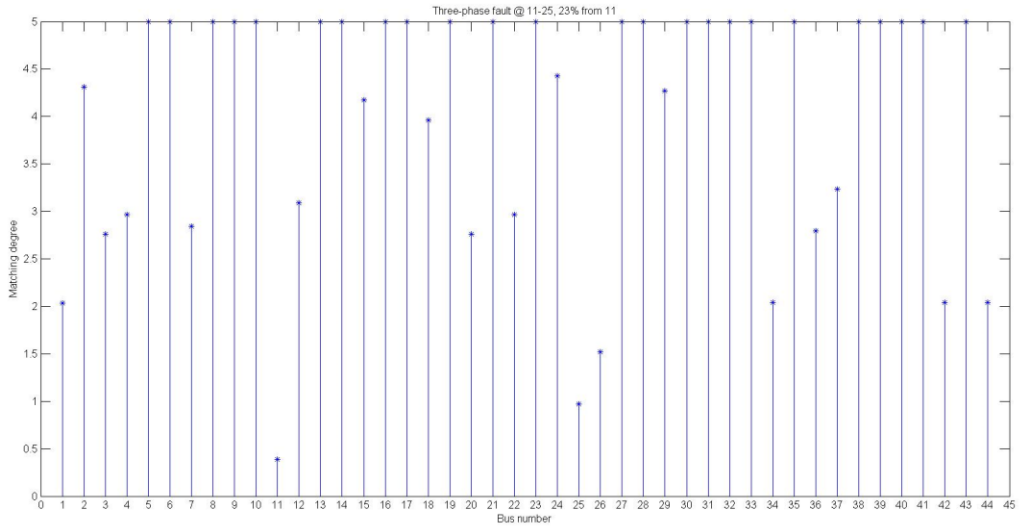

Figure 4. 5: Three-phase fault on line 11-25, 23% from 11.

Based on Figure 4.5, bus 11 and bus 25 should be selected as the suspicious fault buses. To ensure accuracy, bus 26, 34, 42, 44 should be selected as suspicious fault buses as well.

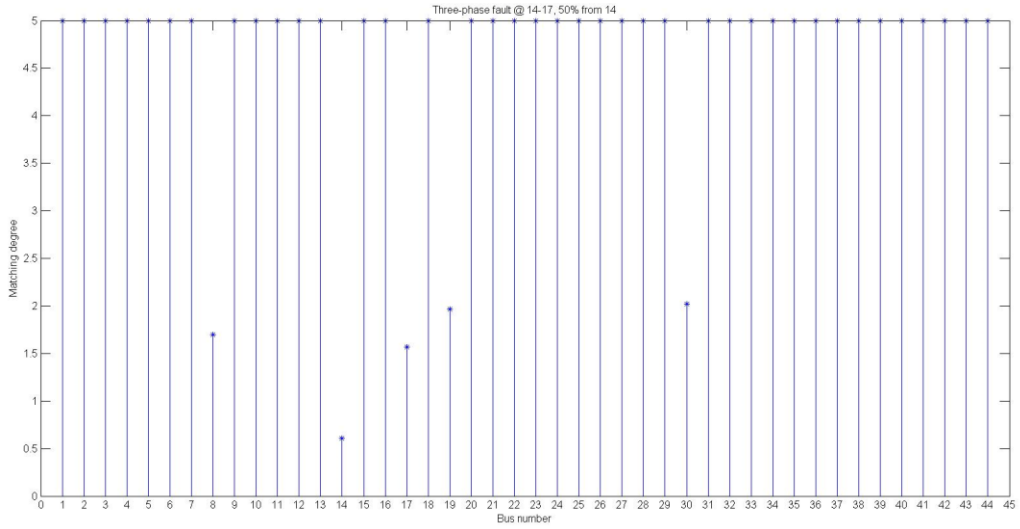

Figure 4. 6: Three-phase fault on line 14-17, 50% from 14.

From Figure 4.6, bus 14 and bus 17 are selected as suspicious fault buses.

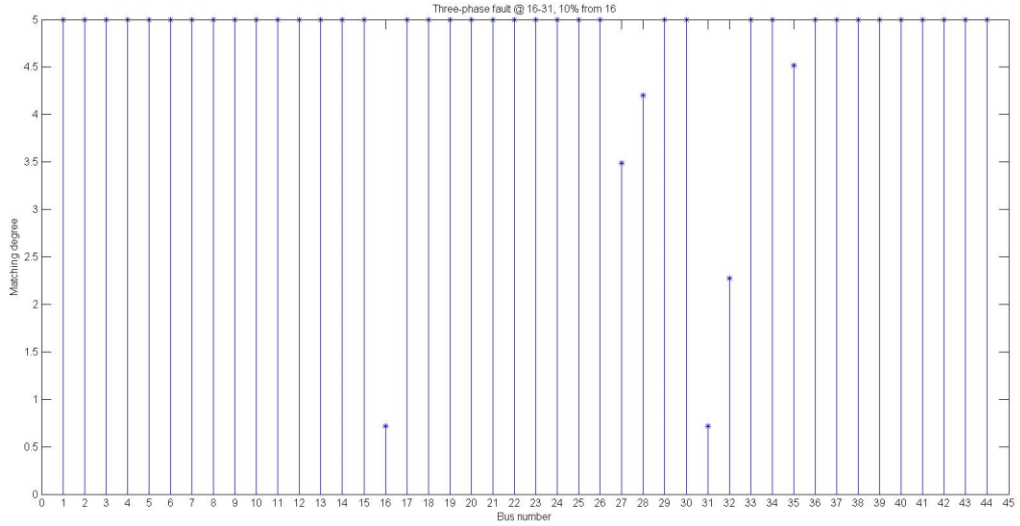

Figure 4. 7: Three-phase fault on line 16-31, 10% from 16.

Bus 16 and bus 31 are the suspicious fault buses since they have the two minimum δ values based on Figure 4.7.

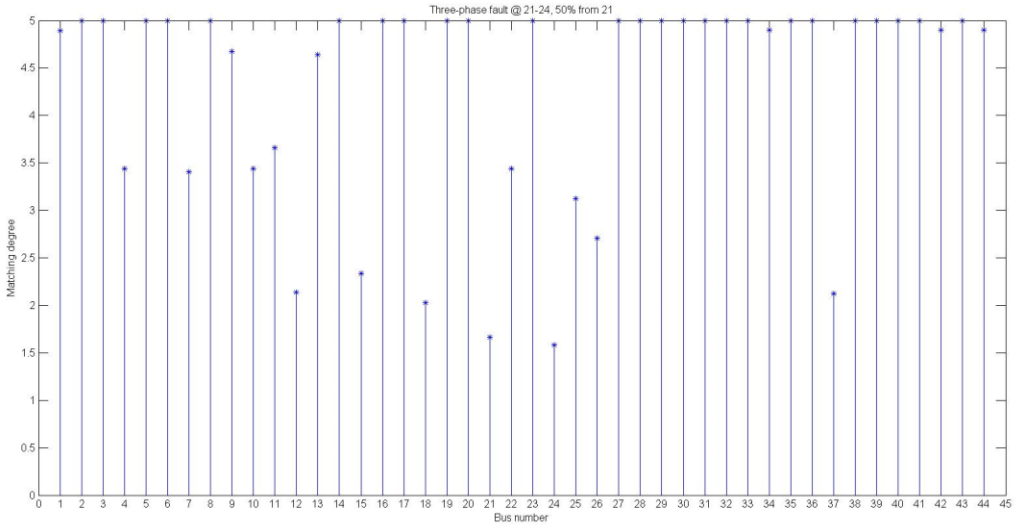

Figure 4. 8: Three-phase fault on line 21-24, 50% from 21.

In Figure 4.8, bus 21 and bus 24 have the two minimum δ values. However, some other buses that also have relatively small delta such as bus 18, 12, 37 and 15 should be selected as suspicious fault buses.

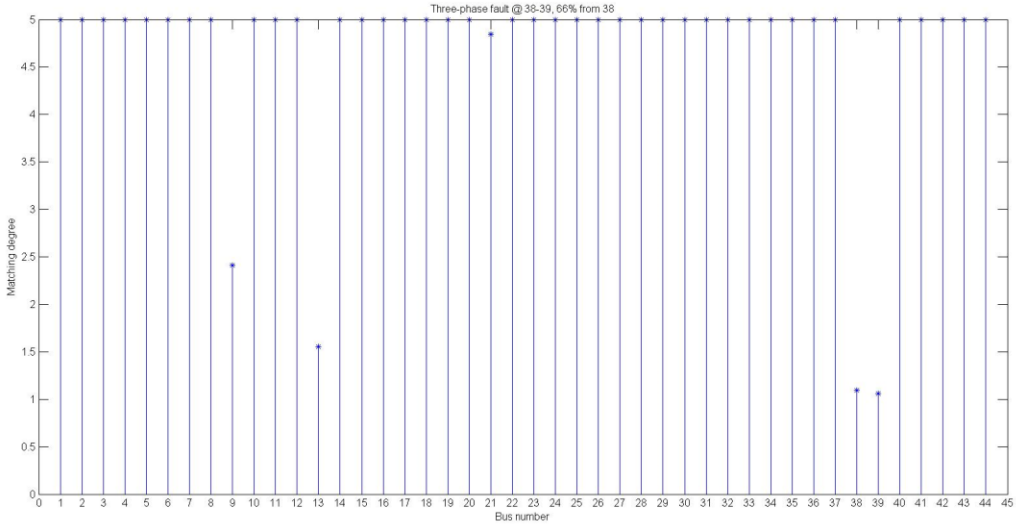

Figure 4. 9: Three-phase fault on line 38-39, 66% from 38.

In Figure 4.9, bus 38 and bus 39 have the two minimum δ values. These two buses are the suspicious fault buses. Figures 4.2 to 4.9 show that the algorithm can successfully identify the suspicious fault buses for three-phase fault on various transmission lines.

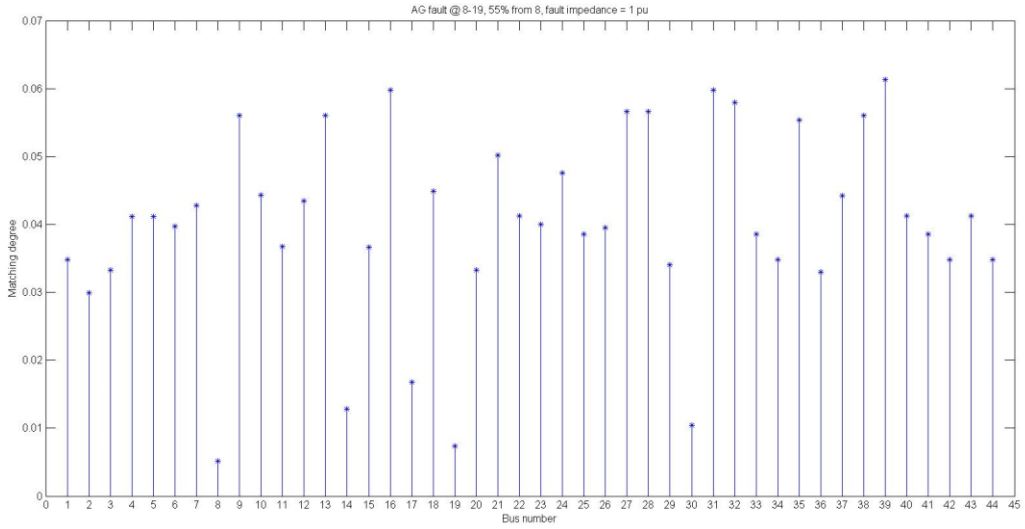

Figure 4. 10: AG fault on line 8-19, 55% from 8, Z_f=1 p.u.

From Figure 4.10, bus 8 and bus 19 have the two minimum δ values. So they are selected as the suspicious fault buses. Besides, bus 14, 17 and 30 also have relatively small δ values, they should be selected as suspicious fault buses as well.

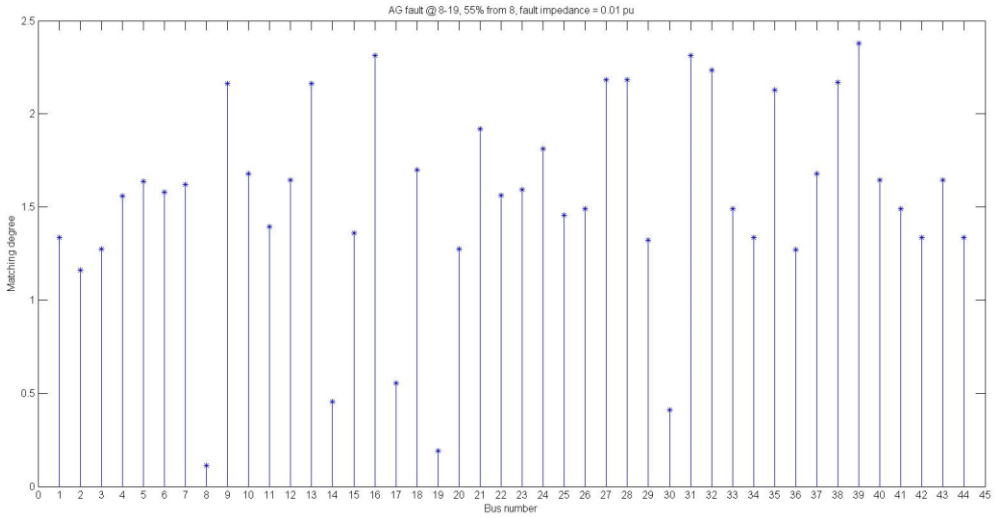

Figure 4. 11: AG fault on line 8-19, 55% from 8, Z_f=0.01 p.u.

Based on Figure 4.11, bus 8 and bus 19 still have the two minimum δ values when the fault impedance is changed from 1p.u to 0.01p.u. When compare Figure 4.11 to Figure 4.10, the overall shapes are similar, only the vertical scale goes up when decreasing the fault impedance.

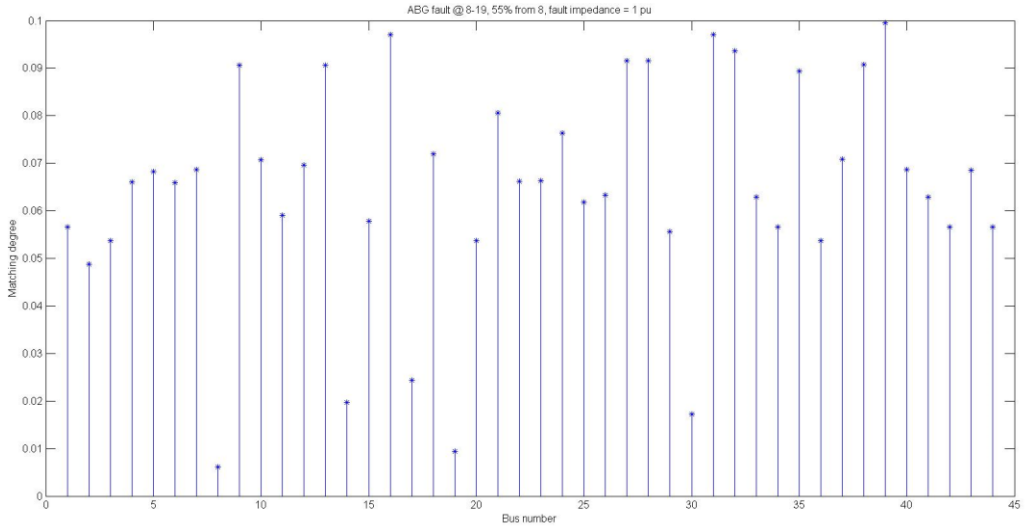

Figure 4. 12: ABG fault on line 8-19, 55% from 8, Z_f=1 p.u.

From Figure 4.12, bus 8 and bus 19 are selected as the suspicious fault buses. Compare Figure 4.12 to Figure 4.10, the algorithm is able to identify the suspicious fault buses when fault type is changed from AG fault to ABG fault under the same fault impedance.

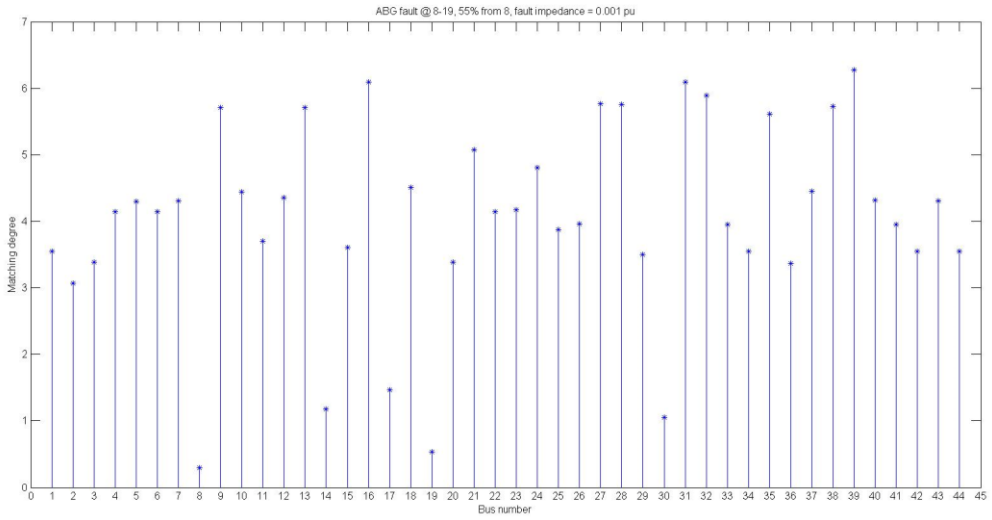

Figure 4. 13: ABG fault on line 8-19, 55% from 8, Z_f=0.001 p.u.

From Figure 4.13, bus 8 and bus 19 still have the two minimum δ values. Compare Figure 4.13 to Figure 4.12, when the fault impedance is changed from 1p.u to 0.001p.u under the same fault type (ABG), the algorithm is still able to identify the correct suspicious fault buses.

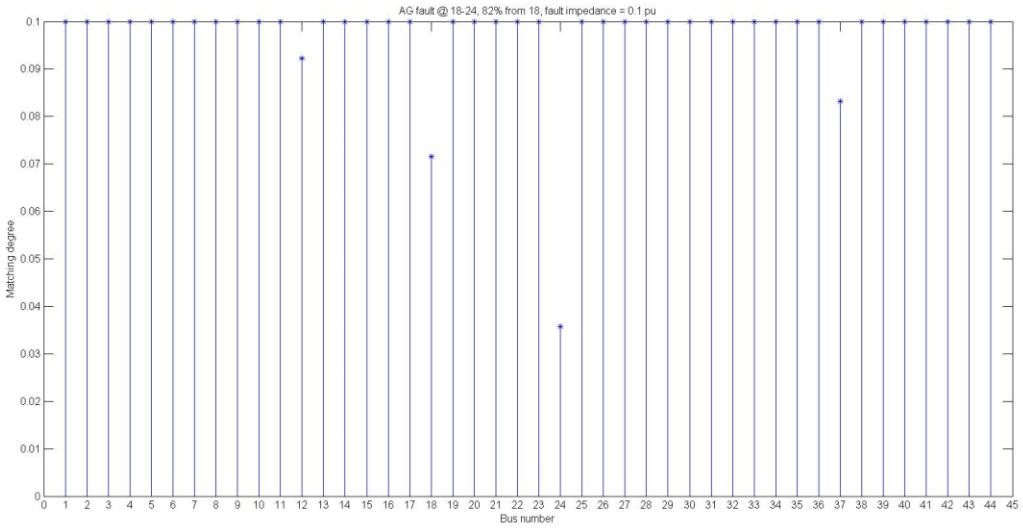

Figure 4. 14: AG fault on line 18-24, 82% from 18, Z_f=0.1 p.u.

Based on Figure 4.14, bus 18 and bus 24 have the two minimum δ values for AG fault with fault impedance 0.1p.u. Therefore, these two buses are the suspicious fault buses.

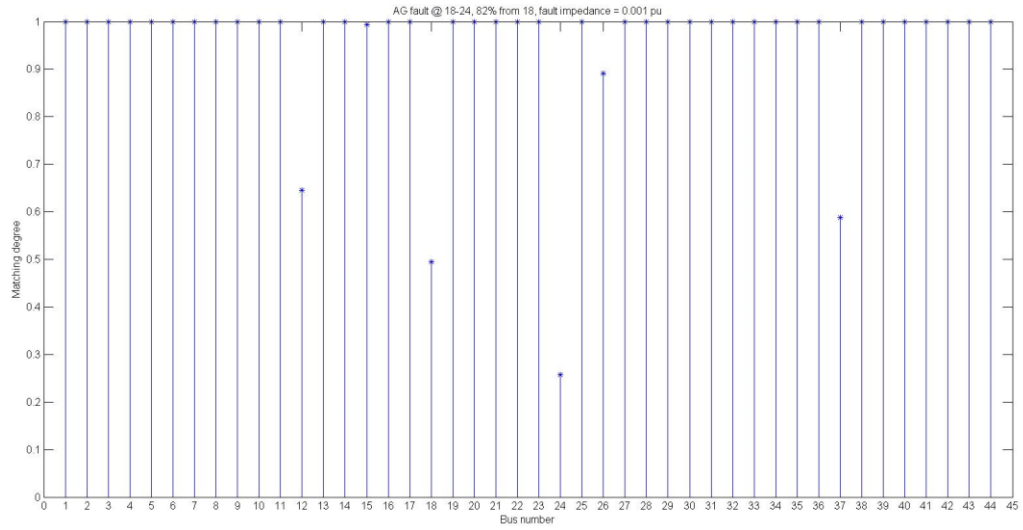

Figure 4. 15: AG fault on line 18-24, 82% from 18, Z_f=0.001 p.u.

Based on Figure 4.15, bus 18 and bus 24 still have the two minimum δ values. Compare Figure 4.15 to Figure 4.14. It is obvious that when the fault impedance is changed from 0.1p.u to 0.001p.u, under the same fault type (AG fault), the algorithm results are not affected.

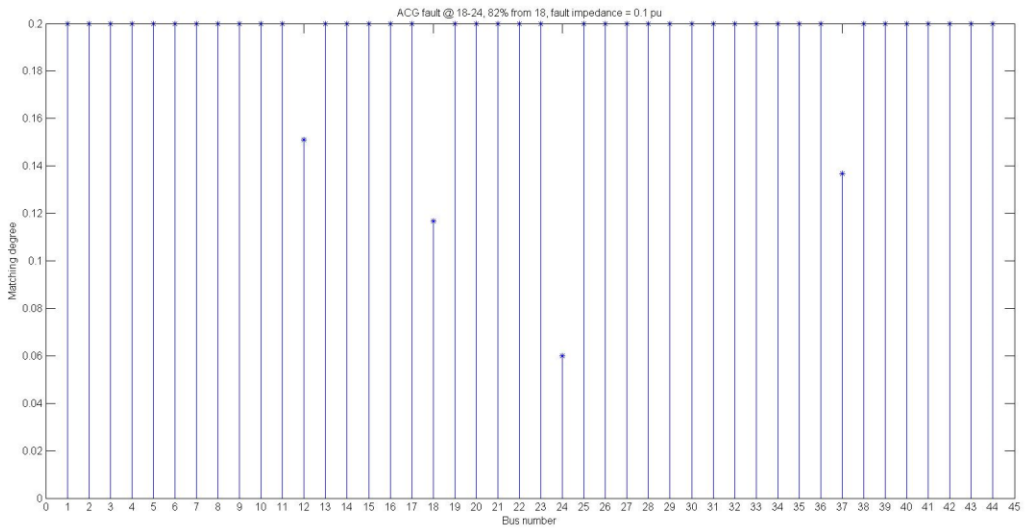

Figure 4. 16: ACG fault on line 18-24, 82% from 18, Z_f=0.1 p.u.

In Figure 4.16, bus 18 and bus 24 have the two minimum δ values for ACG fault with $Z_f = 0.1\ p.u$. Compare Figure 4.16 to Figure 4.14, with the same fault impedance (0.1p.u), when the fault type is changed from AG to ACG, the algorithm is still able to identify the suspicious fault buses.

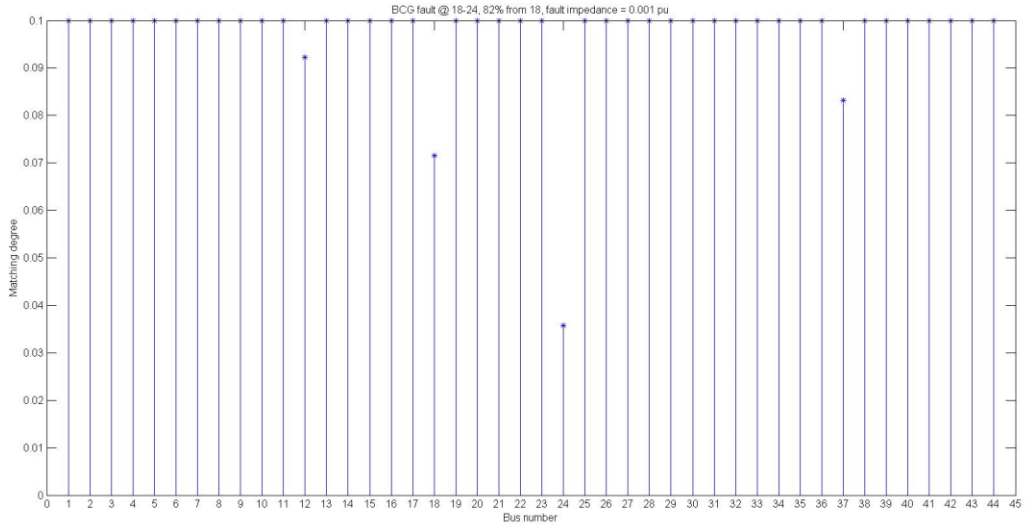

Figure 4. 17: BCG fault on line 18-24, 82% from 18, Z_f=0.001 p.u.

In Figure 4.17, bus 18 and bus 24 still have the two minimum δ values. Compare Figure 4.17 to Figure 4.15, it is easy to see that when the fault resistance keeps the same (0.001p.u), and the fault type is changed from AG to BCG, this algorithm is still able to find the suspicious fault buses.

- **Implement the algorithm on the 44-bus system and verify the stage 2**

To verify the stage 2 of the algorithm, each transmission line has been tested. Table 1 below shows the estimated fault locations for the same 16 lines as previous section under different fault types, fault resistance.

Tested Lines	**Actual Fault Location**	**Fault Type**	**Fault Resistance (p.u)**	**Estimated Fault Location**	**Calculated δ values**	**Fault Location Error (ε)**
2-29	75% from 2	3 – Φ	-	75.16% from 2	0.9223	0.16%
9-27	47% from 9	3 – Φ	-	47.27% from 9	0.9550	0.27%
10-15	15% from 10	3 – Φ	-	15.33% from 10	0.1023	0.33%
11-25	23% from 11	3 – Φ	-	12.97% from 11	0.3626	0.03%
14-17	50% from 14	3 – Φ	-	49.77% from 14	0.2304	0.23%
16-31	10% from 31	3 – Φ	-	10.42% from 16	0.5408	0.42%

21-24	50% from 21	$3-\Phi$	-	50.00% from 21	0.6822	0.00%
38-39	66% from 38	$3-\Phi$	-	66.19% from 38	0.8249	0.19%
8-19	55% from 8	AG	1	55.07% from 8	0.0084	0.07%
8-19	55% from 8	AG	0.01	55.23% from 8	0.1633	0.23%
8-19	55% from 8	ABG	1	54.79% from 8	0.0096	0.21%
8-19	55% from 8	ABG	0.001	54.68% from 8	0.4756	0.32%
18-24	82% from 18	AG	0.1	82.29% from 18	0.0330	0.29%
18-24	82% from 18	AG	0.001	82.40% from 18	0.2321	0.40%
18-24	82% from 18	ACG	0.1	81.62% from 18	0.0552	0.38%
18-24	82% from 18	BCG	0.001	82.29% from 18	0.0330	0.29%

Table 7: Algorithm implementation results for stage 2.

From table 7, it is easy to observe that the Two-Stage fault location algorithm has been successfully implemented on this practical 500kv, 44-bus transmission network. For different types of faults, different fault resistance, the algorithm is able to estimate the fault locations with a maximum error 0f 0.42% which is a pretty good accuracy compare to those One-terminal, Multi-terminal methods. The implementation resualts also imply that this algorithm won't be affected by the fault type and fault resistance.

4.3 Summary

In this chapter, the Two-Stage fault location algorithm has been adapted for implementation on a real 500kv transmission network which has 44 buses. The stage 1 of the algorithm is verified by calculating the matching degree δ values for all buses, and selecting several suspicious fault buses that have relatively smaller δ values. Usually, one should be able to find two δ values are significantly smaller than the rest, those two buses can be selected as the suspicious fault buses. In some cases, even though one may find two minimum δ values, but they are not significantly larger than other buses' δ values, in this case, all the buses that have relatively small δ values should be selected as the suspicious fault buses. All the testing results show that the algorithm is able to find the fault buses. And for most cases, the two buses where the fault is between can be identified directly in stage 1.

The stage 2 of the algorithm is verified by first selecting the possible fault lines, followed by updating the fault distance on that line and calculating all the matching degree δ values for each update on each possible fault line. The minimum δ value, and its corresponding distance x is the estimated fault distance on the selected line.

All results show that this algorithm can be incorporate to a PMU only linear state estimator to provide a fast, independent, and reliable fault location indicator at the control center.

Chapter 5: Conclusion and Future Scope of Work

5.1 Conclusion

Fault location detection is a crucial area in power system. Locating the fault faster and accurately is important for the correct normal operation of the power system and for situational awareness at the control room. With the development of PMUs and the application of the linear state estimator for the control center, the need arises for a fault location method that can be adapted to the system observability set of PMUs used on a linear state estimator. The major contribution of this work is the implementation of a transfer impedance based two-stage fault location algorithm based on the original work of Dr. Jiang [14] and the adaption to work with data available form a PMU only linear state estimator. Unlike classic fault location methods, this method can be implemented with the observability set of PMUs that must be installed for linear state estimator. The required calculations can be programmed into the central data concentrator and the method is not affected by the fault types and fault resistance. The method has been tested using several standard IEEE systems and their results verify the effeteness of the method. A practical 500kV 44-bus, with PMU placement for linear state estimator implementation is used to evaluate the performance of the proposed two-stage fault location algorithm, and the results show that this algorithm is able to locate the fault with an acceptable error.

Another valuable contribution in this thesis is to provide a detailed derivation of the two-stage fault location algorithm which was not covered originally in [14]. Besides, a problem with the derivation of the post-fault system impedance matrix proposed by the authors in [14] was pointed out, and the solution to the problem was also presented in the thesis. Therefore, the integrated, clear two-stage fault location algorithm presented in this work can be used to work with any practical deployment of PMUs for linear state estimator.

5.2 Future Scope of work

All test cases in chapter 3 used the PSS/E simulated post fault voltages which assume to be the real PMU fault voltage measurements. In reality, PMU measurements contain some errors such as total vector error (TVE). The effect of the PMU fault voltage measurements error on the algorithm remains to be evaluated. Since usually the TVE is $\leq 1\%$, a random magnitude and phase error with less than 1% based on the simulated voltages can be utilized to test this algorithm.

Instrument transformers such as CTs and PTs also provide some errors during real applications. The effect of this errors has to be take into account, therefore, simulations that involves those errors need to be performed. Note that these errors are present in most fault location packages commercially available.

With the availability of Open PDC and its ability to implement additional functions on the PMU data, translating the developed Matlab code to C# and adapting to the Open PDC environment needs to be performed for full field implementation.

In this thesis, the two-stage fault location algorithm only analyzed the positive sequence network. However, the improvement of utilizing not only the positive sequence network, but also the negative sequence and zero sequence networks on accuracy of the algorithm still remains to be evaluated.

Appendix A: Verification of the key claim in Two-Stage fault location algorithm

Appendix A.1

In chapter 3, section 3.2.1, a claim is made that the closer to the fault point the smaller the matching degree δ will be. This aforementioned claim is the core of this algorithm, and it is worth to prove it. Now consider a simple example from [32]. In a 3-bus system, a three-phase fault occurs at bus 2, the one line diagram is shown in Figure A.1.

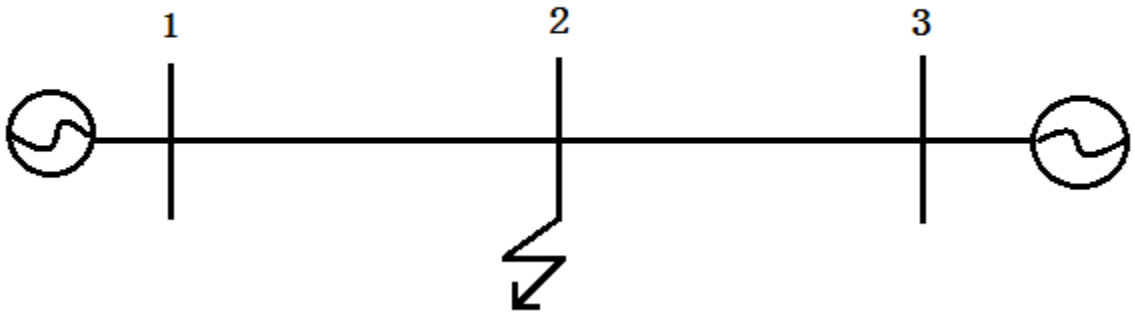

Figure A. 1: Simple 3-bus system with a three-phase fault on bus 2.

The bus impedance matrix of this 3-bus system is: $Z = j\begin{bmatrix} 0.12 & 0.08 & 0.04 \\ 0.08 & 0.12 & 0.06 \\ 0.04 & 0.06 & 0.08 \end{bmatrix}$ in per unit.

The pre-fault bus voltages are assumed to be 1.0 per unit. When a three-phase fault occurs at bus 2, the post-fault bus voltages are given by:

$$V_1^{post} = 0.3333\ V$$

$$V_2^{post} = 0\ V$$

$$V_3^{post} = 0.5\ V$$

Thus, the voltage difference at each bus can be calculated as following,

$$\Delta V_1 = 0.333 - 1 = -0.6667\ V \quad \text{……(A.1.1)}$$

$$\Delta V_2 = 0 - 1 = -1\ V \quad \text{……(A.1.2)}$$

$$\Delta V_3 = 0.5 - 1 = -0.5\ V \quad \text{……(A.1.3)}$$

Assume the fault occurs at bus 1, thus, the matching degree δ_1 needs to be calculated by using (3.2.17). To calculate δ_1, K_1, K_2 and K_3 should be calculated first (assuming fault is on bus 1),

$$K_1 = \left|\frac{\Delta V_1}{Z_{11}}\right| = 5.5556 \quad \text{……(A.1.4)}$$

$$K_2 = \left|\frac{\Delta V_2}{Z_{21}}\right| = 12.5 \quad \text{……(A.1.5)}$$

$$K_3 = \left|\frac{\Delta V_1}{Z_{31}}\right| = 12.5 \quad \text{……(A.1.6)}$$

$\overline{K}$ is the average value of K_1, K_2 and K_3,

$$\overline{K} = \frac{1}{3}\sum_{i=1}^{3} K_i = \frac{1}{3}(5.5556 + 12.5 + 12.5) = 10.1852 \quad \text{……(A.1.7)}$$

$$\delta_1 = \sqrt{\frac{1}{3}\sum_{i=1}^{3}[K_i - \overline{K}]^2} \cong 3.2736 \quad \text{……(A.1.8)}$$

Now, assume fault occurs on bus 2. Calculate the matching degree δ_2 by using the same procedure when calculate δ_1,

$$K_1 = \left|\frac{\Delta V_1}{Z_{12}}\right| = 8.3338 \quad \text{……(A.1.9)}$$

$$K_2 = \left|\frac{\Delta V_2}{Z_{22}}\right| = 8.3333 \quad \text{……(A.1.10)}$$

$$K_3 = \left|\frac{\Delta V_3}{Z_{32}}\right| = 8.3333 \quad \text{……(A.1.11)}$$

$$\overline{K} = \frac{1}{3}\sum_{i=1}^{3} K_i = \frac{1}{3}(8.3338 + 8.3333 + 8.3333) = 8.3335 \quad \text{……(A.1.12)}$$

$$\delta_2 = \sqrt{\frac{1}{3}\sum_{i=1}^{3}[K_i - \overline{K}]^2} \cong 0.0002 \quad \text{……(A.1.13)}$$

Finally, assume the fault occurs at bus 3, calculate δ_3 using the same method when calculating δ_1 and δ_2,

$$K_1 = \left|\frac{\Delta V_1}{Z_{13}}\right| = 16.6667 \quad \text{……(A.1.14)}$$

$$K_2 = \left|\frac{\Delta V_2}{Z_{23}}\right| = 16.6667 \quad \text{……(A.1.15)}$$

$$K_3 = \left|\frac{\Delta V_3}{Z_{33}}\right| = 6.25 \quad \text{……(A.1.16)}$$

$$\overline{K} = \frac{1}{3}\sum_{i=1}^{3} K_i = \frac{1}{3}(16.6667 + 16.6667 + 6.25) = 13.1945 \quad \text{……(A.1.17)}$$

$$\delta_3 = \sqrt{\frac{1}{3}\sum_{i=1}^{3}[K_i - \overline{K}]^2} \cong 4.91 \quad \text{……(A.1.18)}$$

From previous calculations, it is easy to see that δ_2 is the minimum value which is also very close to zero. Hence, it indicates that the fault point is on bus 2 which is the true according to the example statement. Therefore, this simple example could prove the aforementioned claim that the matching degree δ is the minimum value (and close to zero) only at the fault point.

Appendix A.2

In Figure A.2, a three-phase fault occurs at 80% from bus G, the pre-fault voltages at bus G and bus H are $V_G = 1\angle 0^0$, $V_H = 1\angle -30^0$. The fault resistance $Z_f = 0.09 p.u.$ During fault currents I_G, I_H, I_F and the line impedance Z_1 are given in per unit.

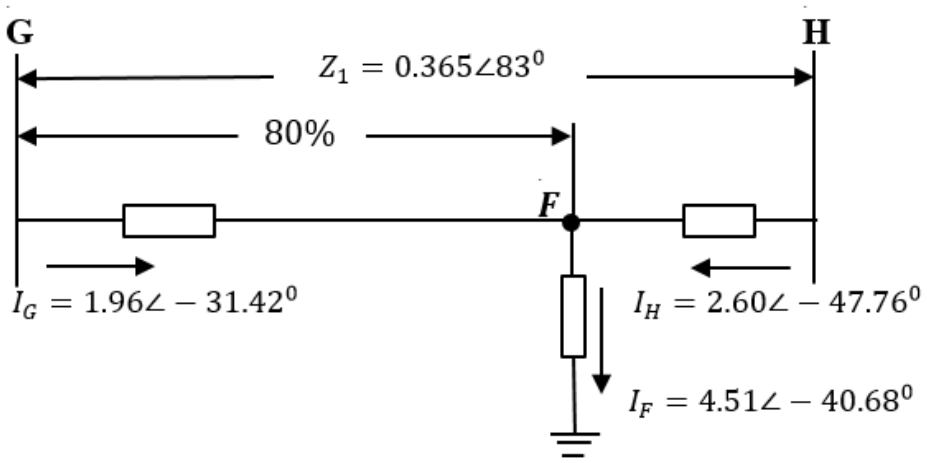

Figure A. 2: A simple 2-bus system with a fault occurs 80% from G-end [37]. ([37] J. D. L. Ree, ECE 4354 Exam #2 Problem 2, Power System Protection Course, Virginia Tech, April. 2014. Used under fair use, 2015)

During fault, the voltages at bus G and bus H can be calculated as following:

$$V_f = I_F * Z_f = 0.4059\angle -40.68° \ p.u. \quad \text{.....(A.2.1)}$$

$$V_G = I_G * 0.8 * Z_1 + V_f = 0.6885\angle 15.49° \ p.u. \quad \text{.....(A.2.2)}$$

$$V_H = I_H * 0.2 * Z_1 + V_f = 0.4881\angle -18.52° \ p.u. \quad \text{.....(A.2.3)}$$

Now, the voltage difference at bus G and bus can be obtained,

$$\Delta V_G = 0.6885\angle 15.49° - 1\angle 0^0 = 0.38347\angle 151.347^0 \ p.u. \quad \text{.....(A.2.4)}$$

$$\Delta V_H = 0.4881\angle -18.52° - 1\angle -30^0 = 0.530663\angle 139.451^0 \ p.u. \quad \text{.....(A.2.5)}$$

Assume the generator impedance at bus G and bus H are:

$Z_G = 0.1 + j0.2 \ p.u.$, $Z_H = 0.05 + j0.15 \ p.u.$

Now, the system admittance matrix Y and impedance matrix Z can be derived as equation (A.2.6) and (A.2.7) below,

$$Y = \begin{bmatrix} 2.3339 - j6.7193 & -0.3339 + j2.7193 \\ -0.3339 + j2.7193 & 2.3339 - j8.7193 \end{bmatrix} \quad \text{……(A.2.6)}$$

$$Z = \begin{bmatrix} 0.0584 + j0.1465 & 0.0237 + j0.0416 \\ 0.0237 + j0.0416 & 0.0375 + j0.1185 \end{bmatrix} \quad \text{……(A.2.7)}$$

Assume the fault is at bus G, the matching degree at bus G $\delta_G = 4.36$ can be calculated by using equations (3.2.17), (3.2.19) and (3.2.20).

Apply the same logic for bus H, $\delta_H = 1.19$. In this example, the fault is 80% from bus G. From the calculations, the matching degree $\delta_G = 4.36$, which is larger than δ_H. By doing this, the claim that "the closer to the fault the smaller the δ value will be" has been proved.

For the case that fault is 80% from bus G, we can update the system admittance matrix Y and impedance matrix Z as following,

$$Y = \begin{bmatrix} 2.4174 - j7.3991 & -0.4174 + j3.3991 \\ -0.4174 + j3.3991 & 0.4174 - j3.3991 \end{bmatrix} \quad \text{……(A.2.8)}$$

$$Z = \begin{bmatrix} 0.1 + j0.2 & 0.1 + j0.2 \\ 0.1 + j0.2 & 0.1356 + j0.4898 \end{bmatrix} \quad \text{……(A.2.9)}$$

Again, by using equations (3.2.17), (3.2.19) and (3.2.20), we can calculate $\delta_{80\%} = 0.336$, which is close to zero and much smaller than δ_G and δ_H. Thus, the claim that "at the exact fault location, the matching degree δ has the minimum value, which should be close to zero" has been proved.

Appendix B: IEEE 9-bus System Data

Line parameter (all lines have the same parameters for simplicity) of the system is shown in Table 8 below:

	R (Ω/km)	**X (mho/km)**	**G (mho/km)**	**B (mho/km)**
Positive Sequence	0.0357	0.5077	0	3.271e-6
Zero Sequence	0.03631	0.1326	0	2.322e-6

Table 8: Line parameter data for IEEE 9-bus system.

Generator positive- and zero-sequence impedance are shown in Table 9,

Generator bus #	**Positive Sequence (Ω)**	**Zero Sequence (Ω)**
1	0.155+j5.95	1.786+j7.58
2	0.238+j6.19	0.833+j5.12
3	0.42+j5.95	1.785+j7.54

Table 9: Generator impedance data for IEEE 9-bus system.

Load data is shown in Table 10,

Load bus #	**P (MW)**	**Q (MVAR)**
5	30	20
6	30	20
8	30	20

Table 10: Load data for IEEE 9-bus system.

Appendix C: IEEE 39-bus System Data

The system branch and transformer data are shown in Table 11,

From Bus	To Bus	R (p.u)	X (p.u)	B (p.u)	Transformer wind ratio (p.u)
1	2	0.0035	0.041	0.6987	0
1	39	0.001	0.025	0.75	0
2	3	0.0013	0.0151	0.75	0
2	25	0.007	0.0086	0.146	0
2	30	0	0.0181	0	1.0250
3	4	0.0013	0.0213	0.2214	0
3	18	0.0011	0.0133	0.2138	0
4	5	0.0008	0.0128	0.1342	0
4	14	0.0008	0.0112	0.1382	0
5	8	0.0008	0.0112	0.1476	0
6	5	0.0002	0.0026	0.0434	0
6	7	0.0006	0.0092	0.113	0
6	11	0.0007	0.0082	0.1389	0
6	31	0	0.025	0	1.07
7	8	0.0004	0.0046	0.078	0
8	9	0.0023	0.0363	0.3804	0
9	39	0.001	0.025	1.2	0
10	11	0.0004	0.0043	0.0729	0
10	13	0.0004	0.0043	0.0729	0
10	32	0	0.02	0	1.07
11	12	0.0016	0.0435	0	1.006
12	13	0.0016	0.0435	0	1.006
13	14	0.0009	0.0101	0.1723	0
14	15	0.0018	0.0217	0.366	0
16	17	0.0007	0.0089	0.1342	0
16	19	0.0016	0.0195	0.304	0
16	21	0.0008	0.0135	0.2548	0
16	24	0.0003	0.0059	0.068	0
17	18	0.0007	0.0082	0.1319	0
17	27	0.0013	0.0173	0.3216	0
19	33	0.0007	0.0142	0	1.07
19	20	0.0007	0.0138	0	1.06
20	34	0.0009	0.018	0	1.009
21	22	0.0008	0.014	0.2565	0
22	23	0.0006	0.0096	0.1846	0
22	35	0	0.0143	0	1.025
23	24	0.0022	0.035	0.361	0
23	36	0.0005	0.0272	0	1

25	26	0.0032	0.0323	0.513	0
25	37	0.0006	0.0232	0	1.025
26	27	0.0014	0.0147	0.2396	0
26	28	0.0043	0.0474	0.7802	0
26	29	0.0057	0.0625	1.029	0
29	38	0.0008	0.0156	0	1.025

Table 11: Branch and Transformer data for IEEE 39-bus system [38]. ([38] Carr, Katie. IEEE 39-Bus System, Illinois Center for a Smarter Electric Grid (ICSEG), Information Trust Institute, 2 Oct. 2013. Web. <http://publish.illinois.edu/smartergrid/ieee-39-bus-system/>. Used under fair use, 2015)

The system bus data and load data is shown in Table 12,

Bus #	**Bus Type***	**Voltage (p.u)**	**Angle (degree)**	**PGen (MW)**	**QGen (MW)**	**Pload (MW)**	**Qload (MW)**
1	1	1.048	-9.43	0	0	0	0
2	1	1.0505	-6.89	0	0	0	0
3	1	1.0341	-9.73	0	0	322	2.4
4	1	1.0116	-10.53	0	0	500	184
5	1	1.0165	-9.38	0	0	0	0
6	1	1.0172	-8.68	0	0	0	0
7	1	1.0067	-10.84	0	0	233.8	84
8	1	1.0057	-11.34	0	0	522	176
9	1	1.0322	-11.15	0	0	0	0
10	1	1.0235	-6.31	0	0	0	0
11	1	1.0201	-7.12	0	0	0	0
12	1	1.0072	-7.14	0	0	8.5	88
13	1	1.0207	-7.02	0	0	0	0
14	1	1.0181	-8.66	0	0	0	0
15	1	1.0194	-9.06	0	0	320	153
16	1	1.0346	-7.66	0	0	329	32.3
17	1	1.0365	-8.65	0	0	0	0
18	1	1.0343	-9.49	0	0	158	30
19	1	1.0509	-3.04	0	0	0	0
20	1	0.9914	-4.45	0	0	628	103
21	1	1.0377	-5.26	0	0	274	115
22	1	1.0509	-0.82	0	0	0	0
23	1	1.0459	-1.02	0	0	247.5	84.6
24	1	1.0399	-7.54	0	0	308.6	-92.2
25	1	1.0587	-5.51	0	0	224	47.2
26	1	1.0536	6.77	0	0	139	17
27	1	1.0399	-8.78	0	0	281	75.5
28	1	1.0509	-3.27	0	0	206	27.6
29	1	1.0505	-0.51	0	0	283.5	26.9
30	2	1.0475	-4.47	250	104.75	0	0
31	3	0.9820	0.00	650	98.31	0	0
32	2	0.9831	1.63	632	99.72	0	0

33	2	0.9972	2.18	508	101.23	0	0
34	2	1.0123	0.74	650	104.93	0	0
35	2	1.0493	4.14	560	106.35	0	0
36	2	1.0635	6.83	540	102.78	0	0
37	2	1.0278	1.26	830	102.65	0	0
38	2	1.0265	6.55	1000	103.00	0	0
39	2	1.0300	-10.96	250	104.75	1104	250

Table 12: Bus and load data for IEEE 39-bus system.

Bus Type*: 1-load bus; 2-generator bus; 3-swing bus

References

[1] Y. Liao, "Fault location utilizing unsynchronized voltage measurements during fault," *Elect. Power Compon. Syst.*, vol. 34, no. 12, pp. 1283–1293, Dec. 2006.

[2] K. Takagi, Y. Yomakoshi, M. Yamaura, R. Kondow, and T. Matsushima, "Development of a new type fault locator using the one-terminal voltage and current data," *IEEE Trans. Power App. Syst.*, vol. PAS-101, no. 8, pp. 2892–2898, Aug. 1982.

[3] D. Novosel, D. G. Hart, E. Udren, and J. Garitty, "Unsynchronized two-terminal fault location estimation," *IEEE Trans. Power Del.*, vol. 11, no. 1, pp. 130–138, Jan. 1996.

[4] A. Gopalakrishnan, M. Kezunovic, S. M. McKenna, and D. M. Hamai, "Fault location using distributed parameter transmission line model," *IEEE Trans. Power Del.*, vol. 15, no. 4, pp. 1169–1174, Oct. 2000.

[5] J.-A. Jiang, J.-Z. Yang, Y.-H. Lin, C.-W. Liu, and J.-C. Ma, "An adaptive PMU based fault detection/location technique for transmission lines—Part I: Theory and algorithms," *IEEE Trans. Power Del.*, vol. 15, no. 2, pp. 486–493, Apr. 2000.

[6] E. G. Silveira and C. Pereira, "Transmission line fault location using two-terminal data without time synchronization," *IEEE Trans. Power Del.*, vol. 22, no. 1, pp. 498–499, Feb. 2007.

[7] A. A. Girgis, D. G. Hart, and W. L. Peterson, "A new fault location technique for two-and three-terminal lines," *IEEE Trans. Power Del.*, vol. 7, no. 1, pp. 98–107, Jan. 1992.

[8] Y.-H. Lin, C.-W. Liu, and C.-S. Yu, "A new fault locator for three-terminal transmission lines—Using two-terminal synchronized voltage and current phasors," *IEEE Trans. Power Del.*, vol. 17, no. 2, pp. 452–459, Apr. 2004.

[9] M. Abe, N. Otsuzuki, T. Emura, and M. Takeuchi, "Development of a new fault location system for multi-terminal single transmission lines," *IEEE Trans. Power Del.*, vol. 10, no. 1, pp. 159–168, Jan. 1995.

[10] S. M. Brahma, "Fault location scheme for a multi-terminal transmission line using synchronized voltage measurements," *IEEE Trans. Power Del.*, vol. 20, no. 2, pt. 2, pp. 1325–1331, Apr. 2005.

[11] C.-W. Liu, K.-P. Lien, C.-S. Chen, and J.-A. Jiang, "A universal fault location technique for N-terminal ($N \geq 3$) transmission lines," *IEEE Trans. Power Del.*, vol. 23, no. 3, pp. 1366–1373, Jul. 2008.

[12] F. H. Magnago, A. Abur "Fault location using wavelets", *IEEE Transactions on Power Del.*, Vol. 13, No.4, October 1998.

[13] C. Y. Evrenosoglu and A. Abur, “Travelling wave based fault location for teed circuits,” *IEEE Trans. Power Del.*, vol. 20, no. 2, pp. 1115–1121, Apr. 2005.

[14] Q. Jiang, X. Li, B. Wang, and H. Wang, “PMU-based fault location using voltage measurements in large transmission networks,” *IEEE Trans. Power Del.*, vol. 27, no. 3, pp. 1644–1652, Jul. 2012.

[15] M. Patel, R.N. Patel, “Fault Detection and Classification on a Transmission Line using Wavelet Multi Resolution Analysis and Neural Network”, *International Journal of Computer Applications (0975-8887)*, vol. 47, no. 22, Jun. 2012.

[16] Jones, Kevin. "Synchrophasor Analytics." *CodePlex*. Dominion Virginia Power, 5 May 2014. Web. 02 May 2015. <http://phasoranalytics.codeplex.com/>.

[17] VYAS, KRIS G., and WALKER A. MATTHEWS, III. *SOUTHERN CALIFORNIA EDISON COMPANY'S (U 338-E) ANNUAL REPORT ON THE STATUS OF SMART GRID INVESTMENTS*. Rep. Rosemead: SOUTHERN CALIFORNIA EDISON, 2014. Print.

[18] D. Spoor, J.G. Zhu: “Improved single-ended traveling-wave fault location algorithm based on experience with conventional substation transducers”, *IEEE Trans. Power Del.*, 2006, 23, (3), pp. 1714– 1720.

[19] P. Jafarian, M. Sanaye-Pasand: “A traveling-wave-based protection technique using wavelet/PCA analysis”, *IEEE Trans. Power Del*., 2010, 25, (2), pp. 588–599.

[20] L. Mili, T. Baldwin, and R. Adapa, “Phasor measurement placement for voltage stability analysis of power systems,” in *Proc. 29th Conf. Dec. Control*, Honolulu, HI, USA, Dec. 5–7, 1990, vol. 6, pp. 3033–3038.

[21] T. L. Baldwin, L. Mili, M. B. Boisen, and R. Adapa, “Power system observability with minimal phasor measurement placement,” *IEEE Trans. Power Syst.*, vol. 8, no. 2, pp. 707–715, May 1993.

[22] John J. Grainger, William D. Stevenson, *Power System Analysis*, New York City, McGraw-Hill, 1994, pp. 195.

[23] Y. Ahn, M. Choi, and S. Kang, "An accurate fault location algorithm for double-circuit transmission system," in Proc. *IEEE Power Engineering Soc. Summer Meeting*, Vol. 3, ppl344-1349, 2000.

[24] Q.C. Zhang, Y. Zhang, and W.N. Song, "Fault location of two-parallel transmission line for non-earth fault using one-terminal data," *IEEE Trans. on Power Del.*, Vol. 14, nNo. 3, pp863-867, Jul. 1999.

[25] Q. Zhang. Y. Zhang, W. Song and Y. Yu, “Transmission line fault location for phase-to-e& fault using one-terminal data”, *IEE Proc. Gener. Trasm. Distrib.,* Vol. 146, 1999, No. 2, pp. 121-124.

[26] M. S. Sachdev, R. Agarwal, “A Technique for Estimating Line Fault Locations from Digital Relay Measurements,” *IEEE Trans. Power Del.,* Vol. PWRD-3, No. 1, Jan 1988, pp. 121-129.

[27] E. Schweitzer, "Evaluation and Development of Transmission Line Fault Locating Techniques Which Use Sinusoidal Steady-State Information," *paper presented to the 9th Annual Western Protective Relay Conference*, Spokane, WA, October, 1982.

[28] V. Cook, "Fundamental aspects of fault location algorithms used in distance protection," Proc. Inst. Elect. Eng. C, vol. 133, no. 6, pp. 354- 368, 1986.

[29] J. S. Thorp, A. G. Phadke, S. H. Horowitz, and M. M. Begovic, “Some applications of phasor measurements to adaptive protection,” *IEEE Trans. Power Syst.*, vol. 3, no. 2, pp. 791–798, May 1988.

[30] M. J.Iskykowski and E.Rosolowski, *Fault Location on Power Network*, New York: Springer, 2010.

[31] "IEEE Guide for Determining Fault Location on AC Transmission and Distribution Lines," *IEEE Std C37.114-2004*, vol., no., pp.1-36, 2005

[32] J. Duncan Glover, Mulukutla S. Sarma, *Power System Analysis and Design*, the University of Michigan, PWS Pub., 1994, pp352.

[33] R. F. Nuqui and A. G. Phadke, “Phasor measurement unit placement techniques for complete and incomplete observability,” *IEEE Trans. Power Del.*, vol. 20, no. 4, pp. 2381–2388, Oct. 2005.

[34] B. Xu and A. Abur, “Observability analysis and measurement placement for system with PMUs,” in Proc. 2004 *IEEE Power Eng. Soc. Conf. Expo.,* Oct. 2004, vol. 2, pp. 943–946.

[35] S. Chakrabarti and E. Kyriakides, “Optimal placement of phasor measurement units for power system observability,” *IEEE Trans. Power Syst.*, vol. 23, no. 3, pp. 1433–1440, Aug. 2008.

[36] B. Gou, “Generalized integer linear programming formulation for optimal PMU placement,” *IEEE Trans. Power Syst.*, vol. 23, no. 3, pp. 1099–1104, Aug. 2008.

[37] J. D. L. Ree, ECE 4354 Exam #2 Problem 2, *Power System Protection Course*, Virginia Tech, April. 2014.

[38] Carr, Katie. *IEEE 39-Bus System*, Illinois Center for a Smarter Electric Grid (ICSEG), Information Trust Institute, 2 Oct. 2013. Web. <http://publish.illinois.edu/smartergrid/ieee-39-bus-system/>.